

# **Lead Free Organometal Halide Perovskites for Photovoltaic Applications**

**M.Sc. Thesis**

By  
**SONAL MITTAL**



**DISCIPLINE OF PHYSICS  
INDIAN INSTITUTE OF TECHNOLOGY  
INDORE  
JUNE 2018**

# Lead Free Organometal Halide Perovskites for Photovoltaic Applications

**A THESIS**

*Submitted in partial fulfillment of the  
requirements for the award of the degree  
of*  
**Master of Science**

*by*  
**SONAL MITTAL**



**DISCIPLINE OF PHYSICS**  
**INDIAN INSTITUTE OF TECHNOLOGY INDORE**  
**JUNE 2018**



# INDIAN INSTITUTE OF TECHNOLOGY INDORE

## CANDIDATE'S DECLARATION

I hereby certify that the work which is being presented in the thesis entitled **LEAD FREE ORGANOMETAL HALIDE PEROVSKITES FOR PHOTOVOLTAIC APPLICATIONS** in the partial fulfillment of the requirements for the award of the degree of **MASTER OF SCIENCE** and submitted in the **DISCIPLINE OF PHYSICS, Indian Institute of Technology Indore**, is an authentic record of my own work carried out during the time period from July 2016 to June 2018 under the supervision of **Dr. Parasharam M. Shirage**, Associate Professor, Discipline of Physics and MEMS.

The matter presented in this thesis has not been submitted by me for the award of any other degree of this or any other institute.

**Signature of the student with date  
(SONAL MITTAL)**

-----  
This is to certify that the above statement made by the candidate is correct to the best of my/our knowledge.

Signature of the Supervisor of  
M.Sc. thesis (with date)  
**(DR. PARASHARAM M. SHIRAGE)**

-----  
**SONAL MITTAL** has successfully given his/her M.Sc. Oral Examination held on **22 June 2018**.

Signature of Supervisor of M.Sc. Thesis  
Date:  
**Dr. Parasharam M. Shirage**

Convener, DPGC  
Date:

Signature of PSPC Member  
**Dr. Ankhi Roy**  
Date:

Signature of PSPC Member  
**Dr. Rupesh Devan**  
Date:

-----



## **Acknowledgements**

Firstly, I would like to express my sincere gratitude to my thesis advisor **Dr. Parasharam M. Shirage** for the continuous support in my M.Sc. project and related research, for his patience, motivation, and immense knowledge.

I would like to thank and express solicit gratitude to our director **Dr. Pradeep Mathur** for providing all facilities and giving me opportunity to work in a nice environment.

I would take the opportunity to express my gratitude to my PSPC members **Dr. Ankhi Roy** and **Dr. Rupesh Devan** for their valuable suggestions.

I am particularly grateful for the assistance given by Dr. Amreen A. Hussain for her valuable and constructive suggestions during the planning and development of this research work. I would like to express my very great appreciation to Mr. Vishesh Manjunath for his willingness to give his time so generously has been very much appreciated.

I would also like to extend my thanks to all AFMRG lab members. I am grateful to all members of AFMRG lab for constant motivation and entertaining discussions. Special note of thanks to Ms. Lichchavi Sinha, Dr. Bhuvaneshwari S. for their support and love throughout project work.

Finally, I must express my very profound gratitude to my parents and to my younger brother Mr. Saurabh for providing me with unfailing support and continuous encouragement throughout my years of study and through the process of researching and writing this thesis. Last but not the least; I would like to thank my friend Mr. Bhavesh for supporting me spiritually throughout my M.Sc. whenever I needed most.



## **Abstract**

Perovskites have risen up the research community in optoelectronic with its propitious applications. More notably in Photovoltaics perovskite has established a platform for researchers over traditional silicon solar cells. Within the last few years, halide perovskites become a very promising photovoltaic material, fascinating the research community. The most efficient devices exceed 22% solar to electrical power conversion efficiency. Where the perovskite emerges as an excellent light absorber. Mostly lead based perovskites have significant efficiency, but leading an environment friendly and more stable photovoltaic research the issues of toxicity of lead and less stability have been considered. A profusion research have been done to replace lead to get nontoxicity and stability, here we have focused on preparing lead free bismuth based organometallic halide perovskite for photovoltaic applications, as it is found that bismuth is more appropriate element for replacement due to its less-toxicity and stability in solar cells.  $(\text{CH}_3\text{NH}_3)_3\text{Bi}_2\text{I}_9$  has been studied by different research community with many possible ways that may enhance its efficiency. Here in this project attempts have been made to prepare methyl-ammonium bismuth iodide (MBI) with combinations of different solvents and different concentrations. To determine the structural, optical and morphological properties of MBI X-ray diffraction (XRD), UV-Visible, and Field Emission Scanning Electron Microscope (FE-SEM) characterizations, respectively, are performed and a comparative analysis have been done. X-ray diffraction pattern studies confirms the formation of phase pure  $\text{TiO}_2$ , perovskite materials. Formation of hexagonal structure oriented along the *c*-axis evidenced the formation of MBI perovskites. The optical characterization confirms the strong visible absorption of MBI with an optical bandgap of 1.69-2.05 eV. To check the stability of MBI XRD and FESEM analysis has been done after intervals of 10 days. Degradation can be seen after 25-30 days in MBI perovskite.

However MBI was identified as a good candidate for the solar cell application due its increased stability than Pb based perovskites. Finally, attempts have been made to fabricate a photovoltaic device using the as-prepared MBI to study its photoresponse. MBI was prepared in different solvents with various concentrations. We have measured efficiency 1.06% for DMSO solvent, 1.77% for DMF+DMSO solvent and finally the highest efficiency 1.87%, we have got with GBL+DMSO solvent. We concluded that GBL+DMSO solvent is best among all three solvents. Stability is also found best with GBL+DMSO solvent. Here we safely conclude that our objective of synthesis of MBI as an alternative to Pb based perovskite solar cell is verified successfully.

## TABLE OF CONTENTS

<b>ABSTRACT.....</b>	<b>i</b>
<b>LIST OF FIGURES.....</b>	<b>v</b>
<b>LIST OF TABLES.....</b>	<b>ix</b>
<b>ABBREVIATIONS.....</b>	<b>xi</b>
<b>1 Introduction</b>	
1.1 Perovskite.....	1
1.1.1 Organic inorganic perovskite.....	4
1.2 Replacement of lead .....	7
1.3 Perovskite in Optoelectronics.....	8
1.3.1 Perovskite in Photovoltaic.....	10
<b>2 Literature Survey</b>	
2.1 Literature survey of perovskites in photovoltaics.....	11
2.2 Literature survey of Lead Free Perovskite Solar cells.....	15
2.3 Motivation of the work .....	16
2.4 Objective.....	17
<b>3 Experimental Techniques</b>	
3.1 Sample Preparation.....	19
3.1.1 Solution based process.....	19
3.1.2 Spin coating.....	21
3.1.3 Cleaning of FTO.....	22
3.1.4 Perovskite coating.....	23
3.1.5 TiO <sub>2</sub> coating.....	24
3.1.6 Fabrication of Solar cell	24
3.2 Characterization Techniques.....	25
3.2.1 XRD.....	25
3.2.1.1 Working principle.....	25
3.2.1.2 Instrumentation.....	26
3.2.2 Scanning Electron Microscopy.....	27
3.2.2.1 Working principle.....	28
3.2.2.2 Instrumentation.....	28
3.2.3 UV-Vis Spectroscopy.....	29
3.2.3.1 Working principle.....	30
3.2.3.2 Instrumentation.....	31
<b>4 Results and Discussion</b>	
4.1 Analysis of perovskite Layer.....	33
4.1.1 XRD analysis of perovskite layer.....	33
4.1.2 FEEM images of perovskite.....	36

4.1.3 UV-Vis analysis of perovskite.....	39
4.1.3.1 UV-Vis analysis of perovskite solution.....	40
4.1.3.2 UV-Vis analysis of perovskite films	40
4.2 Analysis of TiO <sub>2</sub> Layer.....	41
4.2.1 XRD of TiO <sub>2</sub> Layer.....	41
4.2.2 FESEM Image of TiO <sub>2</sub> compact layer	42
4.3 Stability Analysis of MBI perovskite.....	43
4.4 I-V measurements	46
<b>5 Conclusion and Future Scope</b>	
5.1 Conclusion.....	49
5.2 Future studies.....	50
<b>References.....</b>	<b>52</b>

## LIST OF FIGURES

<b>Figure No.</b>	<b>Title</b>	<b>Page No.</b>
1.1	Structure of perovskite $ABO_3$	2
1.2	A,B,X elements in periodic table	5
1.3	Structure of lead based perovskite	6
1.4	Structure of Bismuth based Perovskite	8
1.5	Perovskite solar cell device structure	10
2.1	NREL analysis for photovoltaics	12
3.1	MBI solutions with different solvents and concentrations	20
3.2	Prepared $TiO_2$ solution	21
3.3 (a)	Spin coater	22
3.3 (b)	Inner part of spin coater	22
3.4(a)	Schematic of perovskite coating over FTO	23
3.4 (b)	MBI perovskite film with DMF+DMSO	23
3.4 (c)	MBI perovskite film with GBL+DMSO	23
3.4 (d)	MBI perovskite film with DMSO	23
3.5	Fabrication of solar cell	25
3.6	schematic representation of X-Ray diffraction (Bragg diffraction)	26
3.7 (a)	X-Ray Diffractometer instrumentation	27
3.7(b)	Schematic representation of instrument	27
3.7	Representation of outcomes of incident beam falling on sample in FESEM	28
3.8	Scanning electron microscopy instrumentation	29
3.9	Schematic diagram of UV visible spectroscopy	31
4.1	XRD pattern of MBI perovskite with DMF+DMSO solvent	34

4.2	XRD pattern of MBI perovskite with GBL+DMSO solvent	35
4.3	XRD pattern of MBI perovskite with DMSO solvent	35
4.4	SEM image of MBI with DMF + GBL solvent in 1.5:2.25	37
	(a) concentration	
	(a1) Enlarged image of (a),	
4.4	SEM image of MBI with DMF + GBL solvent in 1.5:1	37
	(b) concentration	
	(b1) Enlarged image of (b)	
4.4	SEM image of MBI with DMF + GBL solvent in 3:2	37
	(c) concentration	
	(c1) Enlarged image of (c)	
4.5	SEM image of MBI with GBL+DMSO solvent in 1.5:2.25	38
	(a) concentration	
	(a1) Enlarged image of (a)	
4.5	SEM image of MBI with GBL+DMSO solvent in 1.5:1	38
	(b) concentration	
	(b1) Enlarged image of (b)	
4.5	SEM image of MBI with GBL+DMSO solvent in 3:2	38
	(c) concentration	
	(c1) Enlarged image of (c)	
4.6	SEM image of MBI with DMSO solvent in 1.5:2.25	39
	(a) concentration	
	(a1) Enlarged image of (a)	
4.6	SEM image of MBI with DMSO solvent in 1.5:1	39
	(b) concentration	
	(b1) Enlarged image of (b)	
4.6	SEM image of MBI with DMSO solvent in 3:2 concentration	39
	(c) (c1) Enlarged image of (c)	
4.7	Absorption spectra for MBI perovskite solutions	40

4.8(a)	Absorption spectra for MBI perovskite Films	41
4.8(b)	Tauc Plot for MBI Perovskite Films	41
4.9	XRD analysis of TiO <sub>2</sub>	42
4.10	FESEM analysis of TiO <sub>2</sub> compact layer	42
4.11(a)	XRD analysis of MBI With DMSO over a period	43
4.11(b)	XRD analysis of MBI With DMF+DMSO over a period	43
4.11(c)	XRD analysis of MBI With GBL+DMSO over a period	43
4.12(a)	SEM image of degraded MBI with DMF+DMSO solvent	45
	(a1)enlarged SEM image of (a)	
4.12(b)	SEM image of degraded MBI with GBL+DMSO solvent	45
	(b1)enlarged SEM image of(b)	
4.12(c)	SEM image of degraded MBI with DMSO solvent	45
	(c1)enlarged SEM image of (c)	
4.13(a)	I-V measurement of MBI perovskite solar cell with DMSO	46
4.13(b)	I-V measurement of MBI perovskite solar cell with DMF+DMSO	46
4.13(c)	I-V measurement of MBI perovskite solar cell with GBL+DMSO	46



## **List of Tables**

**Table 4.1** Stability test of perovskite solar cells with solvents.



# Abbreviations

DMF	Dimethylformamide
DMSO	N, N-Dimethyl Sulfoxide
GBL	$\gamma$ -butyrolactone
ETL	Electron Transport Layer
FTO	Fluorine Doped Tin Oxide
FE-SEM	Field Emission Scanning Electron Microscope
HTM	Hole Transport Material
ITO	Indium Doped Tin Oxide
MAI	Methylammonium Iodide
MBI	Methylammonium Bismuth Iodide
MAPI	Methylammonium Lead Iodide
PCE	Power Conversion Efficiency
PSC	Perovskite Solar Cell
C-Si	Crystalline Silicon



# Chapter 1

## Introduction

---

### 1.1. Perovskite

Perovskite is a large and specific family of compound that has a crystal structure related to mineral perovskite Calcium Titanium oxide ( $\text{CaTiO}_3$ ). The ideal cubic perovskite structure is not very common and also the mineral perovskite itself is slightly distorted. The perovskite family of oxides is probably the best studied family of oxides. The interest in compounds belonging to this family of crystal structures arise in the large and ever surprising variety of properties exhibited and the flexibility to accommodate almost all of the elements in the periodic system. The term perovskite and perovskite structure are often used interchangeably - but while true perovskite (the mineral) is formed of calcium, titanium and oxygen in the form  $\text{CaTiO}_3$ , The name “*Perovskite*” is given by mineralogist L. A. Perovski [1-6]. The typical chemical formula of the perovskite structure is  $\text{ABO}_3$ , where  $A$  and  $B$  denotes two different cations. The ilmenite structure has the same composition as the perovskite one, *i.e.*,  $\text{ABO}_3$  however,  $A$  and  $B$  in this structure are cations of approximately the same size, which occupy an octahedral site. Therefore, though they share the same general chemical formula, structures classified as ilmenite- or ilmenite-related structures (*e.g.*,  $\text{LiSbO}_3$ ) are different from perovskite. Perovskite oxides comprise large families among the structures of oxide compounds, and several perovskite-related structures are currently recognized. Typical

structures consist of large-sized 12-coordinated cations at the *A*-site and small-sized 6-coordinated cations at the *B*-site. Several complex halides and sulfides and many complex oxides have a perovskite structure. In particular, (Mg, Fe) SiO<sub>3</sub> or CaSiO<sub>3</sub> is thought to be the predominant compound in the geosphere [7, 8]. Perovskite compounds with different combinations of charged cations in the *A* and *B*-sites has been observed.

---

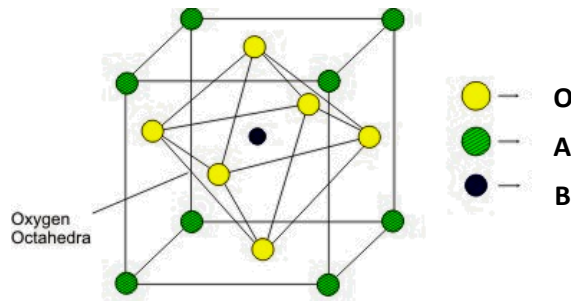


**Figure 1.1:** structure of perovskite ABO<sub>3</sub>

The ideal structure of perovskite, which is illustrated in Fig. 1.1, is a cubic lattice [9]. Although few compounds have this ideal cubic structure, many oxides have slightly distorted variants with lower symmetry (*e.g.*, hexagonal or orthorhombic). Furthermore, even though some compounds have ideal cubic structure, many oxides display slightly distorted variants with lower symmetry. Several examples of perovskite oxides are studied, where it is clear that a large number of perovskite oxides have a rhombohedral lattice.

Additionally, in many compounds a large extent of oxygen or cation deficiency has been observed. Due to the large lattice energy, many compounds are classified as perovskite oxides in spite of the large cation and/or oxygen deficiencies. There are various types of distortions in the perovskite structure that are strongly related to their properties, in particular their ferromagnetic or ferroelectricity. In order to understand the deviations from the ideal cubic structure,

these  $ABO_3$  oxides are first regarded as purely ionic crystals. In the case of the ideal structure, the following relationship between the radii of the  $A$ ,  $B$ , and  $O^{2-}$  ions holds true.

Figure 1.2 shows chemical elements that can be accommodated within the perovskite structure [10]. It is evident that almost all elements except for noble gases can occupy either  $A$  or  $B$  lattice positions in the perovskite structure, including dopants. The stability and the crystal group is mainly determined by the ratio of the ionic radii of the  $A$  and  $B$  cations. Indeed, the structure is dependent not only on the size but also on the nature of the  $A$  and  $B$  atoms.

If we consider perovskite structure in generalized way as  $ABX_3$  then according to availability of  $A, B$  and  $X$  to keep stoichiometry stable We can categorized perovskites as following

- *According to representation of X :*
  - (1) Oxide based Perovskite: as  $A$ ,  $B$  can be fixed either inorganic or organic-inorganic elements but  $X$  is represented as element  $O$  then they are called oxide based perovskites.
  - (2) Halide based Perovskites:  $X$  is represented as Halogen elements and  $A$  and  $B$  may be represented as detailed above in oxide based, then they are called halide perovskites. Halide perovskites are one of the most promising materials for delivery of the next generation of solar cells.
- *According to representation of A and B*
  - (1) Inorganic Perovskite: if all elements  $A$ ,  $B$  and  $X$  is fixed by inorganic elements then it will be categorized under inorganic Perovskites.
  - (2) Hybrid (organic-inorganic) perovskites: In the case of organic–inorganic hybrid perovskites, at least one of the

“A”, “B”, or “X” ions are organic typically, the “A” cation is organic, while “B” is a metal (it can be Pb, Bi, Sn, Ti *etc.*) and “X” is a halogen (Cl, Br, or I), *e.g.*,  $\text{CH}_3\text{NH}_3\text{PbI}_3$  or  $\text{CH}(\text{NH}_2)_2\text{SnI}_3$ , which employ the methylammonium and formamidinium “A” cations, respectively.

Here we are studying broadly hybrid perovskites as an application in optoelectronics.

### 1.1.1 Organic-inorganic perovskites :

Enormous number of experimental and computational efforts have then been devoted to optimizing some halide-based HOIPs, *e.g.*,  $\text{CH}_3\text{NH}_3\text{PbI}_3$ ,  $\text{HC}(\text{NH}_2)_2\text{PbI}_3$ , and  $\text{CH}_3\text{NH}_3\text{SnI}_3$ , for photovoltaic applications. Currently,  $\text{CH}_3\text{NH}_3\text{PbI}_3$  and  $\text{HC}(\text{NH}_2)_2\text{PbI}_3$  have taken a leading position in providing high performance (reaching 20.1% in the conversion efficiency) and low fabrication cost [11].

In fact, there are plenty of choices for the sites A, B, and X in hybrid perovskites. At the site A as an organic methyl ammonium  $\text{CH}_3\text{NH}_3$ , formamidinium  $\text{HC}(\text{NH}_2)_2$  can be substituted and many more have been realized [12]. According to electronic configuration Cations B can be substituted as Lead (Pb), Bismuth (Bi) or Tin (Sn), Titanium (Ti) while the halogens Br, I, and Cl can be used for X. Moreover, the introduction of an organic cation A into the perovskite structure can give raise of many different structural motifs

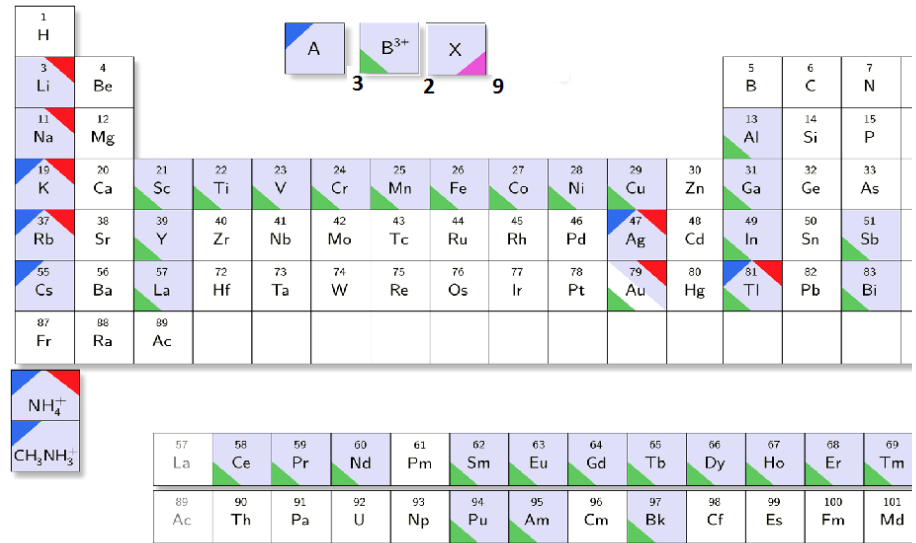


**Figure 1.2:** A,B,X elements in periodic table [12]

Based on the study of major toxicity issue we have broadly divided these perovskites into two categories.

(a) *Lead based perovskite*: when lead is used at B site as a metal then they are called Lead based perovskites. The structure is shown in Fig. 1.3.

Presently  $\text{CH}_3\text{NH}_3\text{PbI}_3$ ,  $\text{HC}(\text{NH}_2)_2\text{PbI}_3$  have been shown as leader in the field of perovskite photovoltaics as efficiency of photovoltaic have been reached till 21% that has brought revolution in this field [13]. But apart from this there are certain limitations which is deviating researchers from the use of lead in perovskite photovoltaics.

Current limitations impeding the commercialization of lead-based halide perovskite solar cells are

- ❖ toxicity
- ❖ bioavailability
- ❖ Probable carcinogenicity of lead and lead halides
- ❖ water solubility of lead that might contaminate water supplies

- ❖ chemical instability under ambient conditions, especially in the presence of air, humidity, and/or light

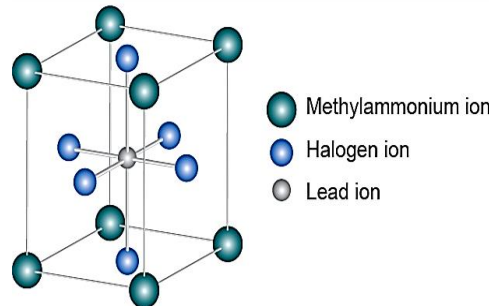


**Figure 1.3:** Structure of lead based perovskite [14]

(b) *Lead free perovskites:* There are so many drawbacks of Lead perovskites even being high efficient for photovoltaic but due to concern of toxicity and stability many researchers had tried to replace lead with other elements which are non-toxic and environmental friendly. Seeking to reduce stability issue and toxicity issue many attempts have been tried to make perovskite materials so that they can be suitable as efficient photovoltaic absorbers.

Because of the fact that the perovskite crystal structure can be found in many compounds, many different material combinations are possible. However, due to these various possibilities, a huge number of materials need to be screened.

This is the drawback that these high efficiencies can only be achieved with lead-based perovskites and this will arguably be a substantial hurdle for various applications of perovskite-based photovoltaics and their acceptance in society, even though the amounts of lead in the solar cells are low. This fact opened up a new research field on lead-free metal halide perovskites, which is currently remarkably vivid [15].

## 1.2 Replacement of Lead:

In recent experimentally and theoretically studies many researchers have tried to replace lead. As reported data and study of electronic configuration states that, we can replace it with Titanium (Ti). Up to now, tin-based perovskites turned out to be most promising in terms of power conversion efficiency; however, also the toxicity of these tin-based perovskites is argued. We can replace it with Germanium (Ge) and Tin (Sn) also but they get oxidized soon so stability issue is here. Although Tin (Sn) based perovskite have been reported to show PCE up to 10 % but the problem associated with it is instability of  $\text{Sn}^{2+}$ , which gets readily oxidized to  $\text{Sn}^{4+}$  when exposed to air [16]. It can be more toxic than lead because oxidation of Sn can cause reaction with organism Alternatively we can replace it with bismuth (Bi) also. In the focus of the research community elements the corresponding perovskite compounds are showing promising properties [17].

### *Bismuth based Perovskite (MBI):*

A site is occupied with methylammonium iodide (MAI) and *B* is occupied with Bi and X is occupied with iodide, then it forms low dimensional structure in  $\text{ABX}_3$  stoichiometry so MBI is found in  $\text{A}_3\text{B}_2\text{X}_9$  stoichiometry as  $\text{MA}_3\text{Bi}_2\text{I}_9$ . The crystal structure is represented in Fig. 1.4.

### Advantages of Bismuth perovskite

- ❖ Reasonable absorption (solar)
- ❖ Less exciton binding energy
- ❖ Less-toxic in comparable with Pb and Sn.
- ❖ Quite stable and reproducible

Over toxicity and stability issue bismuth perovskite can be shown as promising material for photovoltaic application. But there is a drawback in bismuth perovskite as an application in photovoltaic that it

has less efficiency. More work has to be done in this direction. According to previous reported data highest efficiency for MBI has been recorded as 1.64% that is very low as compared to lead perovskite [18].

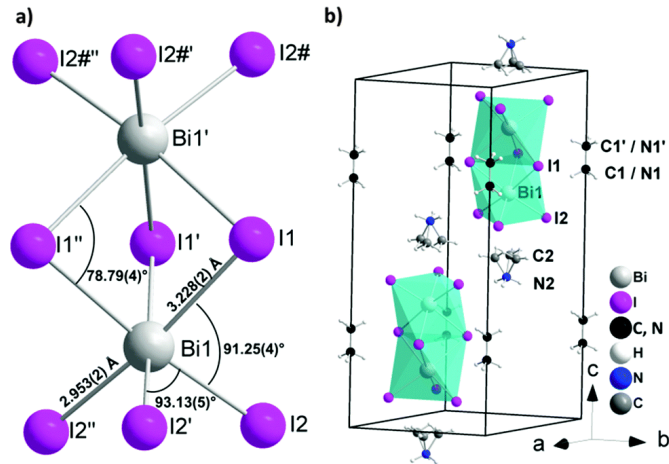


**Figure 1.4:** Structure of Bismuth based Perovskite [19]

### 1.3. Perovskite as an application in Optoelectronics

Perovskite materials have become very promising candidates for a new generation of potentially printable and efficient optoelectronic devices. Recently, hybrid lead halide perovskite photovoltaics have shown an unprecedented evolution from their original publication, reaching efficiencies, which are comparable to *c*-Si in just a few years. This family of materials is easily processable from solution and shows properties comparable to GaAs, making them highly attractive for commercial photovoltaics. Exploring the basic properties of halide-based perovskite materials and their potential for application in optoelectronics, from solar cells to lasers, unique properties of OIHPs are surveyed, including defect physics, ferroelectricity, exciton dissociation processes, carrier recombination lifetime and photon recycling [20].

It is not often that the scientific community is blessed with a material, which brings enormous hopes and receives special

attention. When it does, it expands at a rapid pace and its every dimension creates curiosity. One such material is perovskite, which has triggered the development of new device architectures in energy conversion. Perovskites are of great interest in photovoltaic devices due to their panchromatic light absorption and ambipolar behavior. Power conversion efficiencies have been doubled in less than a year and over 15 % is being now measured in labs. Every digit increment in efficiency is being celebrated widely in the scientific community and is being discussed in industry [21]. Here we provide a summary on the use of perovskite for inexpensive solar cells fabrication. It will not be unrealistic to speculate that one day perovskite-based solar cells can match the capability and capacity of existing technologies. In the recent years, perovskite materials have attracted great attention due to their excellent light-harvesting properties. The organic materials of these hybrid inorganic organic light harvesters are used as sensitizers and the inorganic materials have been used as light absorbers. The exceptional properties of these materials such as long diffusion length, high carrier mobility, affordable device fabrication, and adjustable adsorption range have created a new era in optoelectronic technologies. The perovskites have become promising materials in photovoltaics due to following qualities :

- Their versatility in device architecture
- Flexibility in material growth
- Ability to achieve the high efficiency through various processing techniques.

The superior performance of silicon-based tandems by achieving efficiency more than 40% has encouraged researchers to further expand the investigations to higher levels. The quest to transit the research curiosity to the market photovoltaic technology has given a new dimension to the remarkable ascension of perovskite solar cells [22].

### 1.3.1 Perovskite in photovoltaics :

Here, in this project we are studying perovskite as an application in photovoltaic. The general layer structure for perovskite solar cell is shown in figure 1.5 below. It consists of a transparent electrode, like indium tin oxide (ITO) or fluorine doped tin oxide (FTO), on a glass surface. Here we use FTO coated glass as substrate. In addition, on the ITO/FTO there is an electron-transporting layer (ETL).  $\text{TiO}_2$  is used as an electron transport layer.  $\text{TiO}_2$  behaves like an n-type semiconductor. It separates  $e^-$  that is created in perovskite when light is absorbed. On top of the ETL is the perovskite layer, which is the active layer where the light photon is absorbed and an electron-hole pair (exciton) is excited. On top of the perovskite is the hole-transporting layer (HTL). Spiro-OMeTAD is used as HTM. It separates holes from the junction and lastly a metallic electrode is on the top of HTL. The transparent electrode and the metallic electrode are connected to create a closed circuit cell. When sun light falls upon the junction through transparent electrode solar cell starts working and current flows in external circuit.

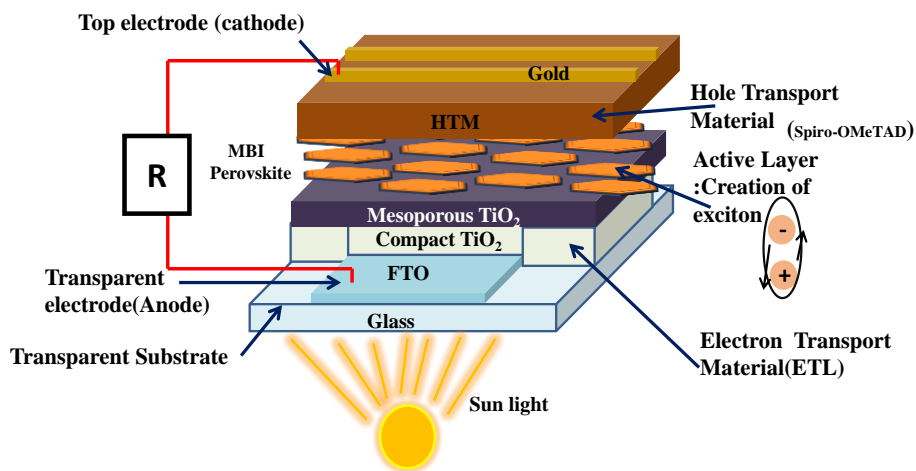


Figure 1.5: Perovskite solar cell device structure

# Chapter 2

## Literature survey

---

---

Perovskites are being used as light harvester since many years. In many fields of optoelectronics perovskites have been emerged as a promising material. Industrialization and population growth around the globe has resulted in exponential increase in demand for energy. According to 2017 statistics India's overall installed capacity has reached 329.4 GW, with renewables accounting for 57.472 GW. Out of which solar energy contributed nearly 19% [23-24]. Seeing this contribution perovskite is being used more in the field of photovoltaics. Since past few years perovskites solar cells have given a hope of significant approach to solve the problems with other types of photovoltaics. So here we have surveyed the performance of perovskite solar cell in last few years. A lot of work has to been in this field.

### **2.1 Literature survey of perovskites in photovoltaics**

These perovskite materials have been well known for many years. Perovskites have been used in optoelectronics as light harvester but in the field of photovoltaics perovskites have taken a revolution since 2009. Over silicon based solar cell perovskite has given a significant contribution in photovoltaics. National Renewable Energy Laboratory (NREL) represents every year analysis of photovoltaics efficiency [25]. According to that, perovskite material has been

emerged as revolutionary part in photovoltaics.

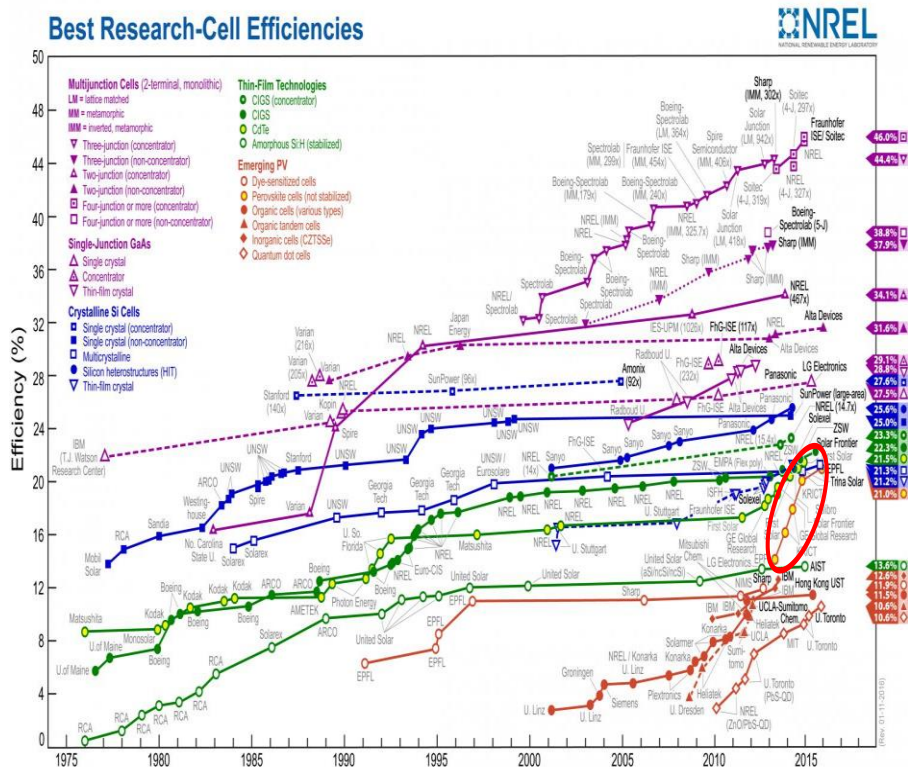


Figure 2.1: NREL analysis for photovoltaics [25]

Figure 2.1 represents efficiency chart for all types of solar cells. Area indicated in red circle represents the progress of perovskite solar cell. Drastically increment in efficiency can be seen in perovskite photovoltaics in last few years. Since past few years perovskite photovoltaics have opened the door for new research in the field of photovoltaics [26].

The first incorporation into a perovskite solar cell was reported by Miyasaka *et al.* in 2009 [27]. This was based on a dye-sensitized solar cell architecture, and generated only 3.8% power conversion efficiency (PCE). In this research, they had used perovskite as a thin layer on mesoporous  $\text{TiO}_2$ . Mesoporous  $\text{TiO}_2$  acts like an electron-collector. They used lead based perovskite  $\text{CH}_3\text{NH}_3\text{PbI}_2$  as an electrolyte. Moreover, because a liquid corrosive electrolyte was used, the cell was only stable for a matter of minutes. Park *et al.*

improved upon this in 2011, they also used the same dye-sensitized concept using perovskite  $\text{CH}_3\text{NH}_3\text{PbI}_2$  nanocrystals using achieving 6.54% PCE [28].

A breakthrough came in 2012, when Henry Snaith and Mike Lee from the University of Oxford realized that the perovskite was stable if it is contacted with a solid-state hole transporter such as spiro-OMeTAD and then it was analyzed that it did not require the mesoporous  $\text{TiO}_2$  layer in order to transport electrons [29, 30]. They showed that efficiencies of almost 10% were achievable using the 'sensitized'  $\text{TiO}_2$  architecture with the solid-state hole transporter, but higher efficiencies, above 10%, were attained by replacing it with an inert scaffold [31]. Further experiments in replacing the mesoporous  $\text{TiO}_2$  with  $\text{Al}_2\text{O}_3$  resulted in increased open-circuit voltage and a relative improvement in efficiency of 3–5% more than those with  $\text{TiO}_2$  scaffolds [32]. This led to the hypothesis that a scaffold is not needed for electron extraction, which was later proved correct. This realization was then closely followed by a demonstration that the perovskite itself could also transport holes, as well as electrons [33]. A thin-film perovskite solar cell, with no mesoporous scaffold, of greater than 10% efficiency was achieved [34, 35].

In 2013, both the planar and sensitized architectures saw a number of developments. Burschka *et al.* demonstrated a deposition technique for the sensitized architecture Using this technique for the fabrication of solid-state mesoscopic solar cells greatly increases the reproducibility of their performance and allows us to achieve a power conversion efficiency of approximately 15% [36].

At a similar time Olga Malinkiewicz *et al.*, and Liu *et al.* showed that it was possible to fabricate planar solar cells by thermal co-evaporation and it was achieved more than 12% and 15% efficiency in a *p-i-n* and an *n-i-p* architecture respectively [37]. They showed

that methyl ammonium lead iodide perovskite layers, when sandwiched between two thin organic charge-transporting layers it leads to higher efficiency, Docampo *et al.* also showed that it was possible to fabricate perovskite solar cells in the typical 'organic solar cell' architecture, an 'inverted' configuration with the hole transporter below and the electron collector above the perovskite planar film they demonstrate that a single thin film of the low-temperature solution-processed organometal trihalide perovskite absorber  $\text{CH}_3\text{NH}_3\text{PbI}_{3-x}\text{Cl}_x$ , sandwiched between organic contacts can exhibit devices with power-conversion efficiency of up to 10% on glass substrates and over 6% on flexible polymer substrates [38].

A range of new deposition techniques and even higher efficiencies were reported in 2014. A reverse-scan efficiency of 19.3% was claimed by Y. Yang at UCLA using the planar thin-film architecture. Zhou *et al.* lowered the defect density of the film by controlling humidity while the perovskite film formed from lead chloride and methylammonium iodide. Low-temperature processing steps allowed the use of materials that draw currents out of the perovskite layer more efficiently [39]. Sang Il Seok and his colleagues at the Korea Research Institute of Chemical Technology blended one of the more well-known perovskite materials– methylammonium lead bromide with a similar compound called formamidinium lead iodide. The researchers say this same blend was responsible for their record-breaking 20.1% efficiency cell, which was confirmed in November 2014 by the US National Renewable Energy Laboratory in Golden, Colorado [40]. The first reported perovskite cell, developed in 2009, yielded an efficiency value of only 3.5%. But since 2012, efficiencies have dramatically improved.

In December 2015, a new record efficiency of 21.0% was achieved

by researchers at EPFL. As of March 2016, researchers from Korea Research Institute of Chemical Technology (KRICT) and UNIST hold the certified record for a single-junction perovskite solar cell with 22.1%. A team of scientists at UNIST had developed a new method for production of inorganic-organic perovskite solar cells, which has achieved record efficiency levels of 22.1%. These efficiencies have been officially confirmed by the U.S. National Renewable Energy Laboratory. Professor Sang-Il Seok at UNIST said “The key to manufacturing high-performance solar cells is to reduce defects in materials that generate energy loss when converting sunlight to electricity”.

In October 2017, a team from Korean Research Institute of Chemical Technology (KRICT) had absorbed the tag of highest achieved 22.7% power conversion efficiency and it is said that it is highest efficiency in world so far in perovskite solar cells.

## **2.2 Literature survey of Lead Free Perovskite solar cells**

One major disadvantage with the  $\text{MAPbX}_3$  perovskite is that it contains lead (Pb), which is rather toxic. An important task is therefore to replace lead in the perovskite, with a different element that is less or non-toxic. Bismuth-based solar cells have exhibited some advantages over lead perovskite solar cells for nontoxicity and superior stability, which are currently two main concerns in the photovoltaic community.

Byung Wook Park *et.al.* reported in 2015 that bismuth based Perovskite can be a promising material in photovoltaics. In his research, he attempted 3 different samples named as  $\text{MA}_3\text{Bi}_2\text{I}_9$ ,  $\text{Cs}_3\text{Bi}_2\text{I}_9$ , and  $\text{MA}_3\text{Bi}_2\text{I}_9\text{Cl}_x$  in order to replace lead and calculated efficiency. With  $\text{Cs}_3\text{Bi}_2\text{I}_9$  Perovskite they had achieved 1.09%

efficiency. Whereas they achieved 0.12% and 0.003% PCE using  $\text{MA}_3\text{Bi}_2\text{I}_9$  and  $\text{MA}_3\text{Bi}_2\text{I}_9\text{Cl}_x$  respectively.

In 2017, Z. Zhang *et.al.* recorded highest efficiency 1.64% so far by using bismuth based perovskite  $\text{MA}_3\text{Bi}_2\text{I}_9$  as light harvester. As an alternative option, bismuth perovskite have been emerged over the issue of toxicity and stability. In organic inorganic bismuth based perovskite it's a highest achieved efficiency so far. Lead perovskite already have achieved a prominent efficiency in photovoltaic but taking into account of environmental issue more research has to be done in the field of lead free perovskite for photovoltaics.

### **2.3 Motivation of the work**

We have analyzed that Lead based Perovskites have come with their outstanding performance in past few years but there are some issue which are unavoidable. Lead perovskite are toxic for environment that is main drawback for lead perovskite. Being toxic, and of lowest stability are of most concerned issues which hinders its commercialization. So as a replacement of lead many attempts have been taken by different groups of researchers. People have tried to replace lead with many elements but those elements were having some issues including stability. Bismuth can be promising material in perovskites for replacement of lead in photovoltaics. More research is being done to improve efficiency of bismuth based organic inorganic perovskites.

Based on vivid literature survey and possible analysis, here in this Project, we are focusing on preparation of lead free organometal halide perovskite solar cell. We are reporting synthesis and characterization of bismuth based organic-inorganic perovskite methyl ammonium bismuth iodide (MBI).

Some research has been done on MBI to make it as a promising perovskite material in order to make lead free perovskite solar cell

feasible. Whereas no proper literature reports preparation of MBI with exact solvents and concentrations to provide better insight in the growth of material. So in this project initially we plan to MBI with definitive solvents and their varied concentrations. A comparative analysis has been done providing information about better material properties suitable for photovoltaic application.

## **2.4 Objectives**

1. Synthesis and characterization of methylammonium bismuth iodide (MBI) with different solvent.
2. Synthesis and characterizations of methylammonium bismuth iodide (MBI) with different concentration.
3. To study the effect of concentration and solvents on the material properties of methylammonium bismuth iodide (MBI).
4. Fabrication of photovoltaic device based on methylammonium bismuth iodide (MBI) and studying the photo-response.



# Chapter 3

## Synthesis and Experimental Techniques

---

---

### 3.1 Sample preparation:

*Materials:* Methylammonium iodides (TCI Chemicals) and Bismuth iodide (Sigma Aldrich) were used as received without any further purification. Dimethylformamide (DMF), Dimethyl sulfoxide (DMSO) and  $\gamma$ -butyrolactone (GBL) have been used as solvent without any further purification. FTO (Fluorine Doped Tin Oxide) coated glasses were used as substrates. Fluorine-doped tin oxide (FTO) coated glass is electrically conductive and ideal for use in a wide range of devices, including applications such as optoelectronics, touch screen displays, thin film photovoltaics, energy-saving windows, Fluorine doped tin oxide has been recognized as a very promising material because it is relatively stable under atmospheric conditions, chemically inert, mechanically hard, high-temperature resistant, has a high tolerance to physical abrasion and is less expensive than indium tin oxide.

#### 3.1.1 Solution based process:

3.1.1 (A) **Perovskite preparation:** In order to make lead free perovskite we have prepared MBI (methylammonium bismuth iodide) perovskite as a solution first with different solvents and concentration so that we can seek in which solvent and concentration photoresponse would be best.

For preparation  $\text{MA}_3\text{Bi}_2\text{I}_9$ , first MAI and  $\text{BiI}_3$  were mixed in three set of experiment with different solvents. In each set three MBI perovskite solutions were made with three different concentrations following each solvent. Combinations of concentrations of MAI and  $\text{BiI}_3$  are following (a) 1.5:1 (b) 2.25:1.5 (c) 3:2.

With these three concentrations, first attempt had been made with a solvent, which was a mixture of certain ratio of DMF and DMSO. Afterwards in next sets of experiment MBI Perovskite solutions were made with same three concentrations in second solvent named DMSO and third set of experiment was done with a solvent that was a solution in certain ratio of GBL and DMSO. All prepared 9 solutions of MBI perovskites were kept for overnight stirring on magnetic stirrer at 1200 rpm at room temperature so that MAI and  $\text{BiI}_3$  can dissolve in solvent properly. The photos of MBI solutions are shown in Fig. 3.1.



**Figure 3.1:** MBI solutions with different solvents and concentrations

3.1.1 (B) **Synthesis of  $\text{TiO}_2$ :** While fabricating photovoltaic device  $\text{TiO}_2$  is used because it acts as electron transport layer due to its high electron affinity and high electron mobility. A compact layer is coated over FTO glass according to device fabrication layout.

Required chemical: titanium diisopropoxide bis (acetylacetonate), 1-butanol.

In order to make a dense TiO<sub>2</sub> compact layer, we have prepared 0.15 M and 0.3 M titanium diisopropoxide bis (acetylacetonate) solution in 1-butanol. The solutions were kept at stirring for overnight. The photo of TiO<sub>2</sub> solution is shown in Fig. 3.2.

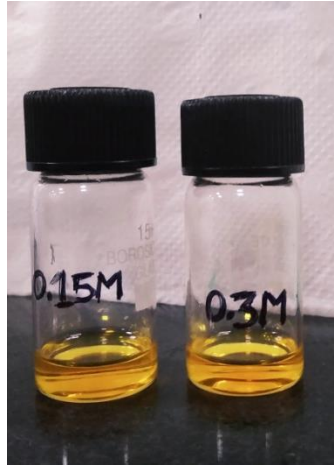


**Figure 3.2:** prepared TiO<sub>2</sub> solution

### **3.1.2 Spin coating :**

Spin coating is one of the most important and common techniques for depositing uniform thin films to flat substrates. This technique is used widely in semiconductor industries, organic electronics and technology sectors. The advantage of spin coating is its ability to quickly and easily produce uniform films; thin film produced by spin coating can range from a few nanometres to a few microns in thickness.

It also has some differences due to the relatively thin films and high uniformity required for effective device preparation, as well as the need for self-assembly and organisation to occur during the casting process.

**Working principle:** Usually a small amount of coating material is applied on the center of the substrate, which is either spinning at low speed or not spinning at all. The substrate is then rotated at high speed in order to spread the coating material by centrifugal force that is acting on substrate radially in outward direction .A machine which is used for spin coating is called a **spin coater**, or simply **spinner**. The photo is shown in Figure 3.3.

Rotation is continued while the fluid spins off the edges of the substrate, until the desired thickness of the film is achieved. The applied solvent is usually vaporescent and simultaneously evaporates. Thickness of the film depends upon speed of spinner. The higher the angular speed of spinning, the thinner the film. The thickness of the film also depends on the viscosity and concentration of the solution, and the solvent.



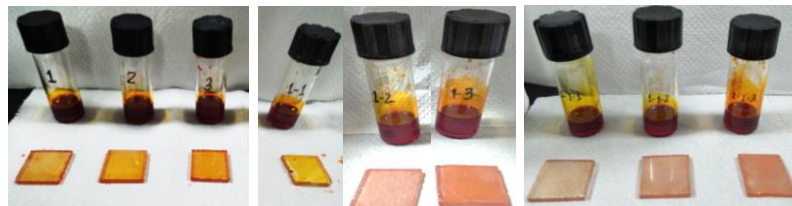
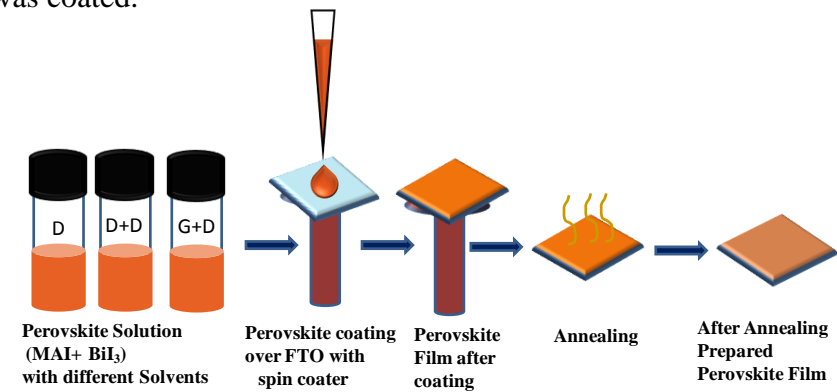
**Figure 3.3:** (a)Spin coater (b) inner part of spin coater

**3.1.3 Cleaning of FTO substrates:** FTO coated glasses were used as a substrate for coating. FTO glasses were purchased in  $18 \times 18$  cm and then they were cut in square shape with fixed dimensions  $2 \times 2$  cm. Cleaning was done in following steps

1. FTO glass is ultrasonicated first with acetone for 10 minute and dried it for 5 minute.

2. In second step FTO is ultrasonicated with isopropanol for 10 minute and dried for 5 minute.
3. At last substrate is sonicated with DI water for 10 minute and we kept it in furnace for 10 minute for drying. These FTO substrates were used for the further coating of solar cell materials.

**3.1.4 Perovskite coating:** We had prepared 9 sample solutions of MBI in 3 sets with different solvents and concentrations. Each MBI perovskite solution was spin coated on FTO glass substrates to make a uniform thin film of perovskite over FTO glasses. 100  $\mu$ ml solution of each solution was dropped on FTO glass with the help of nozzle that is fixed in spin coater with vacuum. After that it was spinned at 3000 rpm speed and 5 sec acceleration for 30 sec. A uniform film of perovskite over FTO glasses was grown. Two layers of each solvent was coated.



(b)

(c)

(d)

**Figure 3.4:** (a) Schematic diagram of Perovskite Coating over substrate, MBI perovskite film with (b) DMF+DMSO (c) GBL+DMSO and (d) DMSO solvents.

**3.1.5 TiO<sub>2</sub> coating:** Solutions were coated on FTO glasses. First, one layer of 0.15M TiO<sub>2</sub> solution was coated on FTO glass and it is dried for 10 min at 125° C. Then two layers of 0.3 M TiO<sub>2</sub> solution was coated followed by annealing at 125° C for 10 Min. Same procedure of coating was done with another FTO glass followed by annealing at 500° for 30 min. Perovskite was coated over this TiO<sub>2</sub> compact Layer while fabricating device.

*Re-preparation of MBI perovskite:* Degradation of MBI perovskites had started after 30 days. So for further measurements MBI perovskites were prepared again with solvents variation (DMSO, DMF: DMSO and GBL: DMSO) with only 3:2 concentration.

### **3.1.6 Fabrication of Solar cell:**

First FTO was cleaned in all prescribed ways as mentioned earlier and then it was etched from sides. After that one side was masked with kapton tap as shown in figure 3.5. Electron transport material was coated over the masked substrate according to earlier mentioned ways. Here we are using TiO<sub>2</sub> as an electron transport layer. TiO<sub>2</sub> layer was annealed at 500°C for 30 minutes. Over the TiO<sub>2</sub> layer MBI perovskite was coated as shown in Figure 3.4(a). After it we keep it at 120°C in furnace for 2 hours. Over the perovskite layer spiro-OMeTAD was coated as hole transport layer (HTM). After annealing masking has to be removed and before coating of each layer masking has to be done again. And finally as top electrode gold was coated over HTM as shown in Figure 3.5. Fabricated solar cell is shown in figure 3.5 with all the steps

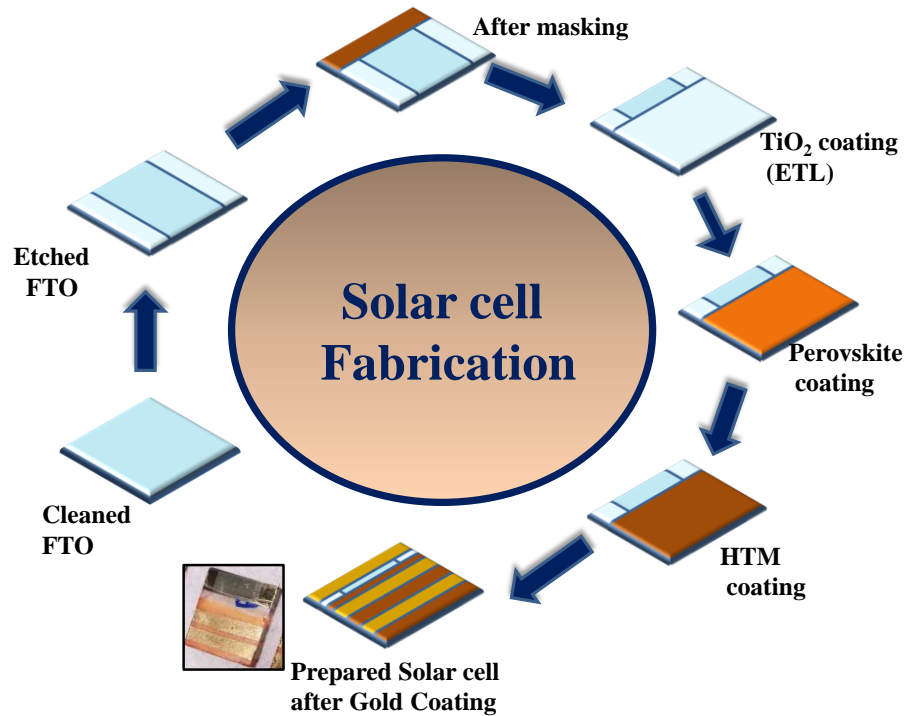


**Figure 3.5 :** Fabrication of Solar cell

### **3.2 Characterization Techniques:**

#### **3.2.1 XRD:**

X-ray powder diffraction (XRD) is a rapid analytical technique which is primarily used for following information's.

- ❖ Phase identification of a crystalline material
- ❖ It can provide information on unit cell dimensions.
- ❖ Measurement of sample purity

X-ray diffraction is now a common technique for the study of crystal structures and phase purity.

*3.2.1.1 Working principle:* X-ray diffraction is based on constructive interference of monochromatic X-rays and a crystalline sample. These X-rays are generated by a cathode ray tube, filtered to produce monochromatic radiation, collimated to concentrate, and directed toward the sample. The relationship between the X-Ray wavelength

( $\lambda$ ), the inter planar distances of the lattice planes  $hkl$ ,  $d_{hkl}$ , and the angle of incident beam to the same set of lattice planes ( $\theta$ ), is given by the Bragg's law.

$$2d_{hkl} \sin\theta = n\lambda$$

Where 'n' is the diffraction order (an integer >0).

The interaction of the incident rays with the sample produces constructive interference (and a diffracted ray) when this condition is satisfied as shown in fig 3.6.

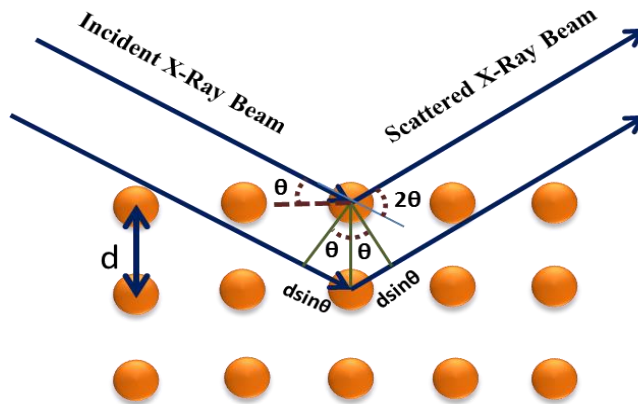


**Figure 3.6** : Schematic representation of X-Ray diffraction (Bragg's diffraction)

### 3.2.1.2 Instrumentation:

X-ray diffractometers consist of three basic elements: an X-ray tube, a sample holder, and an X-ray detector as shown in Fig 3.7. X-rays are generated in a cathode ray tube by heating a filament to produce electrons, accelerating the electrons toward a target by applying a voltage, and bombarding the target material with electrons. When electrons have sufficient energy to dislodge inner shell electrons of the target material, characteristic X-ray spectra are produced. Copper is the most common target material for single-crystal diffraction, with Cu  $K_{\alpha}$  radiation,  $\lambda=1.5418\text{\AA}$ . These X-rays are collimated and directed onto the sample. As the sample and detector are rotated, the

intensity of the reflected X-rays is recorded. When the geometry of the incident X-rays impinging the sample satisfies the Bragg's equation, constructive interference occurs and a peak in intensity occurs. A detector records and processes this X-ray signal and converts the signal to a count rate which is then output to a device such as a printer or computer monitor

The geometry of an X-ray diffractometer is such that the sample rotates in the path of the collimated X-ray beam at an angle  $\theta$  while the X-ray detector is mounted on an arm to collect the diffracted X-rays and rotates at an angle of  $2\theta$ . For typical powder patterns, data is collected at  $2\theta$  from  $\sim 5^\circ$  to  $60^\circ$ , angles that are preset in the X-ray scan.

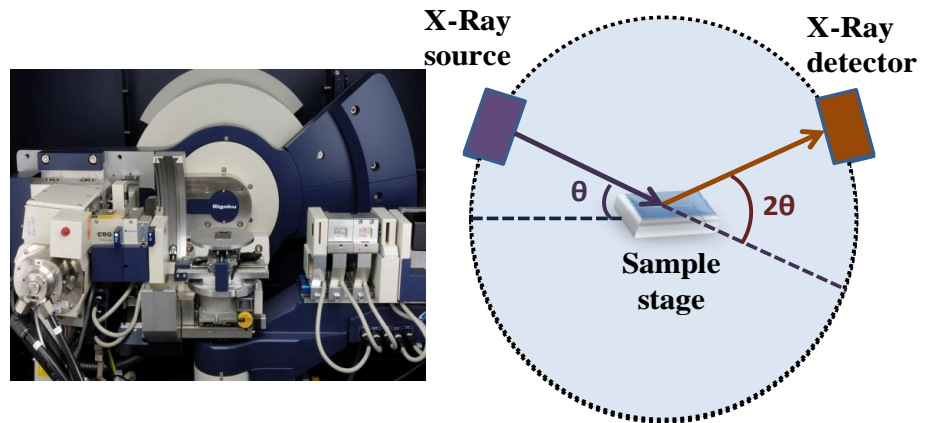


**Figure 3.7:** (a) X-Ray Diffractometer instrumentation [43].  
(b) Schematic representation of instrument.

### 3.2.2 Scanning electron microscope:

Scanning electron microscope is an improved model of an electron microscope. SEM is used to study the three dimensional image of the specimen. A scanning electron microscope (SEM) scans a focused electron beam over a surface to create an image. The electrons in the beam interact with the sample, producing various signals that can be used to obtain information about the surface topography and composition.

### 3.2.2.1 Working principle:

When the accelerated primary electrons strike the sample, it produces secondary electrons. These secondary electrons are collected by a positive charged electron detector which in turn gives a 3-dimensional image of the sample.

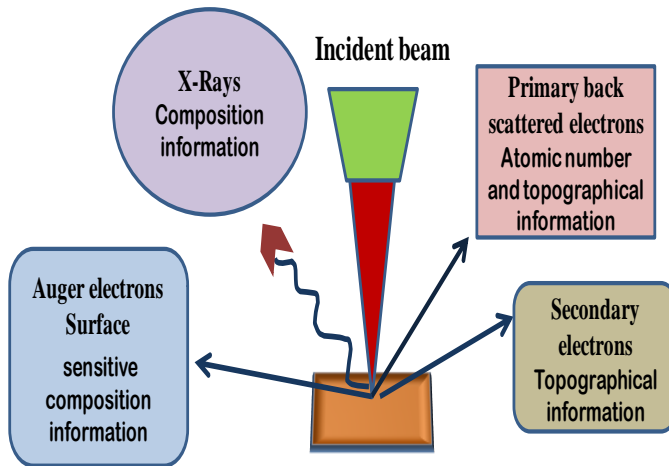


**Figure 3.8:** Representation of outcomes of incident beam falling on sample in FESEM.

**3.2.2.2 Instrumentation:** Electrons are produced at the top of the column, accelerated down and passed through a combination of lenses and apertures to produce a focused beam of electrons, which hits the surface of the sample, as shown in Fig. 3.8 and 3.9. The sample is mounted on a stage in the chamber area and, unless the microscope is designed to operate at low vacuums, both the column and the chamber are evacuated by a combination of pumps. The level of the vacuum will depend on the design of the microscope.

Scan coils situated above the objective lens control the position of the electron beam on the sample. These coils allow the beam to be scanned over the surface of the sample. This beam rastering or scanning, as the name of the microscope suggests, enables information about a defined area on the sample to be collected. As a result of the electron-sample interaction, a number of signals are

produced. Appropriate detectors then detect these signals.

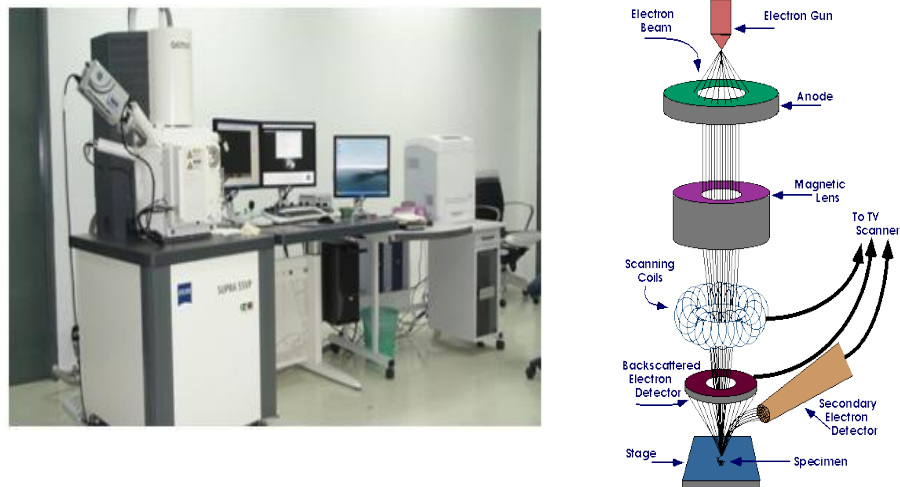


**Figure 3.9:** Scanning electron microscopy instrumentation [44].

### 3.2.3 UV-Vis spectroscopy:

UV-visible spectroscopy (UV-Vis or UV/Vis) involves the spectroscopy of photons in the UV-visible region *i.e.* it uses light in the visible and adjacent (near UV and near infra-red) ranges. The absorption in the visible ranges directly affects the color of the chemicals involved. In this region of the electromagnetic spectrum, molecules undergo electronic transitions. Different molecules absorb radiation of different wavelengths. An absorption spectrum shows a number of absorption bands corresponding to structural groups within the molecule.

**3.2.3.1 Basic principle:** UV spectroscopy obeys the Beer-Lambert's law, which states that: when a beam of monochromatic light is passed through a solution of an absorbing substance, the rate of decrease of intensity of radiation with thickness of the absorbing solution is proportional to the incident radiation as well as the concentration of the solution.

The expression of Beer-Lambert's law is-

$$A = \log (I_0/I) = \epsilon cl$$

Where, A = absorbance

$I_0$  = intensity of light incident upon sample cell

I = intensity of light incident upon sample

C= molar concentration of solute

l= length of sample cell(cm)

$\epsilon$  = molar absorptivity

### **3.2.3.2 Instrumentation:**

UV-Vis spectrometer consists following parts :

(1) Light source (2) monochromator (3) sample and references (4) detector (5) amplifier (6) recording device

Tungsten filament lamps and Hydrogen-Deuterium lamps are most widely used as a suitable light source. It will pass through monochromator and further divided into two beams. One of the two divided beams is passed through the sample solution and second beam is passing through the reference solution. Both sample and reference solution are contained in the cells made by silica not glass (glass absorbs light). Generally, two photocells serve the purpose of detector in UV spectroscopy. One of the photocell receives the beam from sample cell and second detector receives the beam from the reference. The alternating current generated in the photocells is transferred to the amplifier. Generally, current generated in the photocells is of very low intensity, the main purpose of amplifier is to amplify the signals many times so we can get clear and recordable signals. Computer stores all the data generated and produces the spectrum of the desired compound. The schematics of UV-Vis are represented in Figure 3.10.

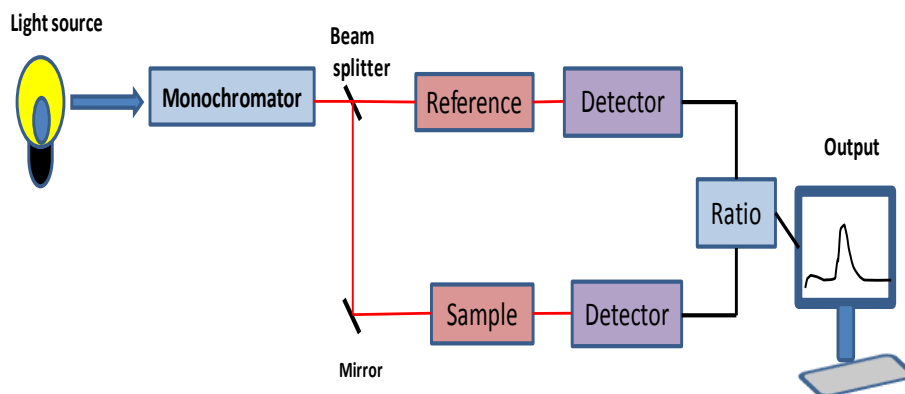


**Figure3.10:** Schematic diagram of UV visible spectroscopy

**3.2.3.3 Tauc Plot:** Tauc *et al.* proposed and substantiated a method for determining the band gap using optical absorbance data plotted appropriately with respect to energy [45, 46]. They show that the optical absorption strength depends on the difference between the photon energy and the band gap as follows

$$\alpha h\nu = B(E_g - h\nu)^m$$

where  $\alpha$  is absorption coefficient,  $\beta$  is an independent constant,  $E_g$  is the energy of the optical band gap and  $m$  is the power factor of the transition mode, which is dependent upon the nature of the material, whether it is crystalline or amorphous. According to Tauc's relation:

$m = 1/2$  for direct allowed transitions

$m = 3/2$  for direct forbidden transitions.

$m = 2$  for indirect allowed transitions

$m = 3$  for indirect forbidden transitions

The plotting of  $(\alpha h\nu)^2$  versus the photon energy ( $h\nu$ ) gives a straight line in a certain region. The extrapolation of this straight line will intercept the ( $h\nu$ )-axis to give the value of the direct optical energy gap ( $E_g$ ).



# Chapter 4

## Results and Discussion :

---

---

Perovskite is being used as a light harvester in optoelectronics. As it is used in photovoltaic device as light absorber, comparison between solvents and concentration for seeking suitable solvent and concentration has been done by characterized samples through XRD for structural property. Furthermore, FESEM images have been analyzed for morphological property. Optical analysis also has been done through UV-Vis spectroscopy. Long term stability analysis has been through XRD and FESEM. Lastly we have analyzed a photoresponse of photovoltaic device.

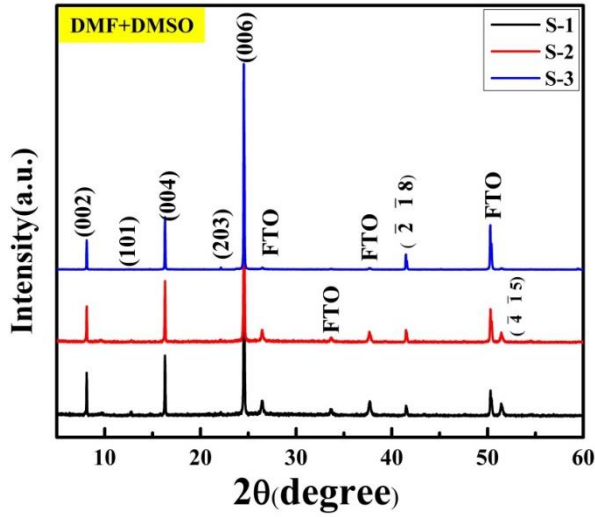
For device fabrication part we have analyzed every layer as they have their own functional role to be a part of photovoltaic device.

### 4.1 Analysis of Perovskite layer

#### 4.1.1 XRD Analysis of MBI Perovskites

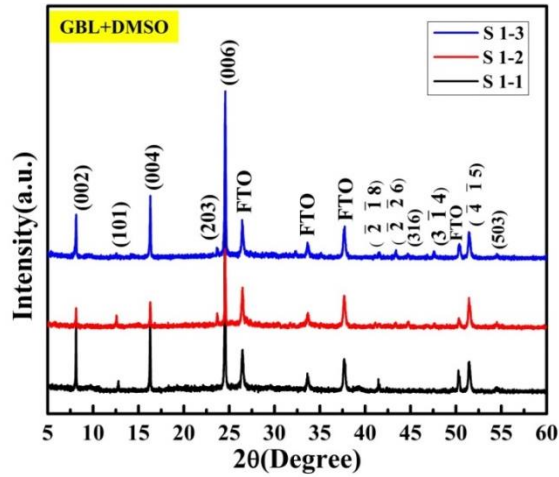
To determine structural properties of MBI perovskites with different solvents and different concentration, X-ray diffraction patterns have been investigated by Rigaku Smartlab. We found various crystalline peaks of MBI which are in good agreement with the literature reports [41]. The crystalline MBI peaks are oriented along the *c*-axis. Crystallographic analysis reveals that the crystal structure of MAPbI<sub>3</sub> belongs to the hexagonal system with the space group P31c (159). We can also see preferred orientation effects of the hexagonal material in such thin films may cause minor differences in the

intensity of the peaks due to substrate (FTO). Summarizing, we have elucidated the correct crystal structure of  $(\text{CH}_3\text{NH}_3)_3\text{Bi}_2\text{I}_9$  using crystal measurements. Although the composition and its applicability for perovskite like hybrid solar cells would suggest similarities to  $\text{CH}_3\text{NH}_3\text{PbI}_3$ , MBI does not contain corner sharing octahedra normally observed in perovskite materials but isolated  $\text{Bi}_2\text{I}_9^{3-}$  anions. With the synthesis procedure described in this study we are able to show, that it is possible to obtain phase pure and highly crystalline  $(\text{CH}_3\text{NH}_3)_3\text{Bi}_2\text{I}_9$  thin films in contrast to previous work [42].



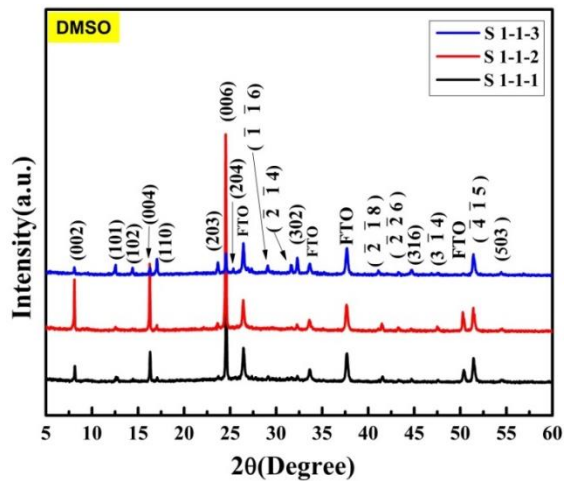
**Figure 4.1:** XRD pattern of MBI perovskite with DMF+DMSO solvent

Figure 4.1 shows the XRD patterns for MBI Perovskites with first solvent (mixture of DMF and DMSO). XRD patterns have been analyzed with this solvent indicating  $c$ - axis growth. We have found that various crystalline peaks of MBI which are in good agreement with the standard JCPDS file no. (01-073-3751). Most of the XRD peaks are oriented along  $c$ -axis indicating the crystalline nature of MBI.



**Figure 4.2:** XRD pattern of MBI perovskite with GBL+DMSO solvent

Figure 4.2 shows the XRD patterns for MBI perovskites with second solvent (mixture of GBL and DMSO). XRD patterns have been analyzed with this solvent also with three different concentrations. Orientations of plane along c- axis and increment in intensity according to concentration have been illustrated with this solvent also.



**Figure 4.3:** XRD pattern of MBI perovskite with DMSO solvent

Figure 4.3 shows the XRD patterns for MBI perovskites with third solvent DMSO. XRD patterns have been analyzed with this solvent

also same as previous two solvents with three different concentrations. Lattice constants were calculated as  $a=b=9.91(\pm 0.002)$  Å and  $c=23.42(\pm 0.004)$  Å using following formula.

$$\frac{1}{d^2} = \frac{4}{3} \left( \frac{h^2 + hk + k^2}{a^2} \right) + \frac{l^2}{c^2}$$

where  $h$ ,  $k$  and  $l$  are the miller indices.

#### 4.1.2 FESEM analysis of MBI Perovskites

Scanning electron microscopy (FESEM) images have been analyzed through Supra55 Zeiss to illustrate the morphological property of MBI perovskite. We illustrate the morphology of the MBI perovskite films prepared via different solvents and different concentrations of MAI and BiI<sub>3</sub>. By analyzing these images, we found the formation of hexagonal crystals of MBI perovskites which are in agreement with the previous reports [43], suggesting that MBI has hexagonal structure with space group P31c (159).

Furthermore, we did a comparative analysis on the morphology of MBI with different solvents as shown in Figure 4.5. With DMSO as the solvent, we found hexagonal crystals oriented in both vertical and horizontal axis. Whereas with DMF + DMSO and  $\gamma$ -butyrolactone + DMSO hexagonal crystals oriented in horizontal axis are prominent. Interestingly a quite dense and uniform morphology of MBI perovskite is found with  $\gamma$ -butyrolactone + DMSO solvent.

From these solvents we can expect to get a better interfacial contact when this material will be integrated in the photovoltaic

device. With some solvents density has been increased with increasing concentration and whereas layer formation can be seen. FESEM images of MBI perovskite samples are shown in Figure 4.4 - 4.6.

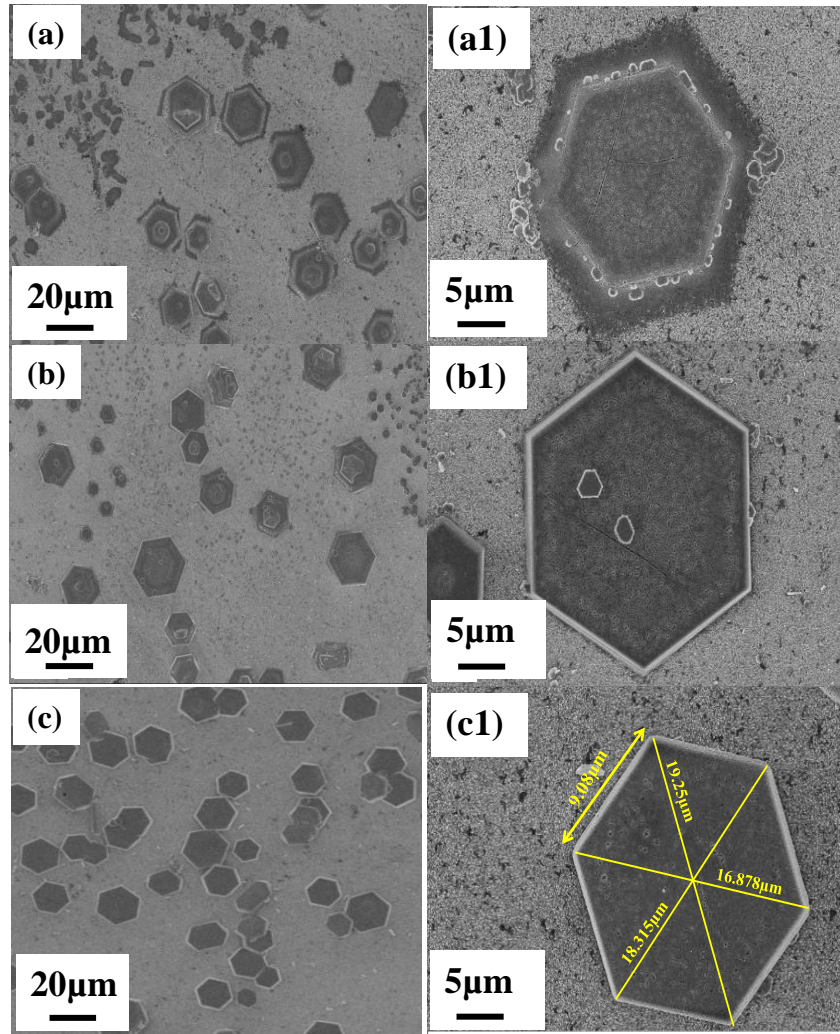


**Figure 4.4** (a) SEM image of MBI with DMF+DMSO solvent in 2.25:1.5 concentration, (a1) Enlarged image of (a), (b) SEM image of MBI with DMF+DMSO solvent in 1.5:1 concentration, (b1) Enlarged image of (b), (c) SEM image of MBI with DMF+DMSO solvent in 3:2 concentration, (c1) Enlarged image of (c)

form. As concentration is being increased layer formation started to grow. In (a) it can be seen that formation of MBI had just started and in (c) it is completed.

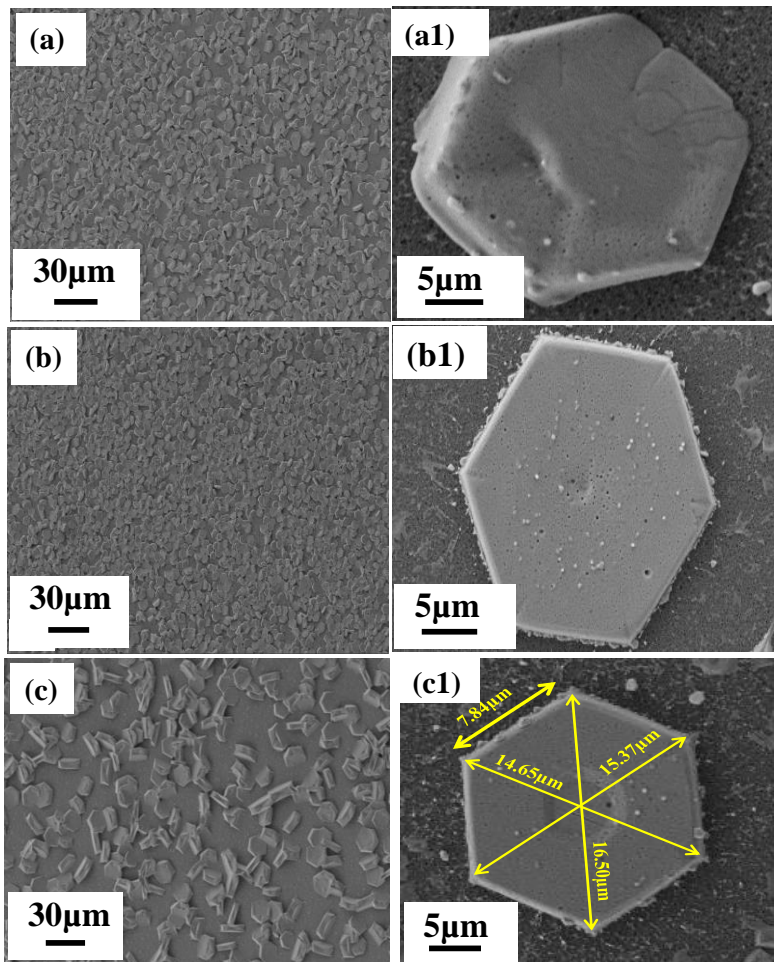


**Figure 4.5** (a) SEM image of MBI with GBL+DMSO solvent in 2.25:1.5 concentration, (a1) Enlarged image of (a), (b) SEM image of MBI with GBL+DMSO solvent in 1.5:1 concentration, (b1) Enlarged image of (b), (c) SEM image of MBI with GBL+DMSO solvent in 3:2 concentration, (c1) Enlarged image of (c)

Figure 4.5 shows morphology of MBI perovskite with (GBL+DMSO) solvent which shows that increasing concentration is

causing increasing density. With most increased density we will find more compact interfacial contact in device fabrication.

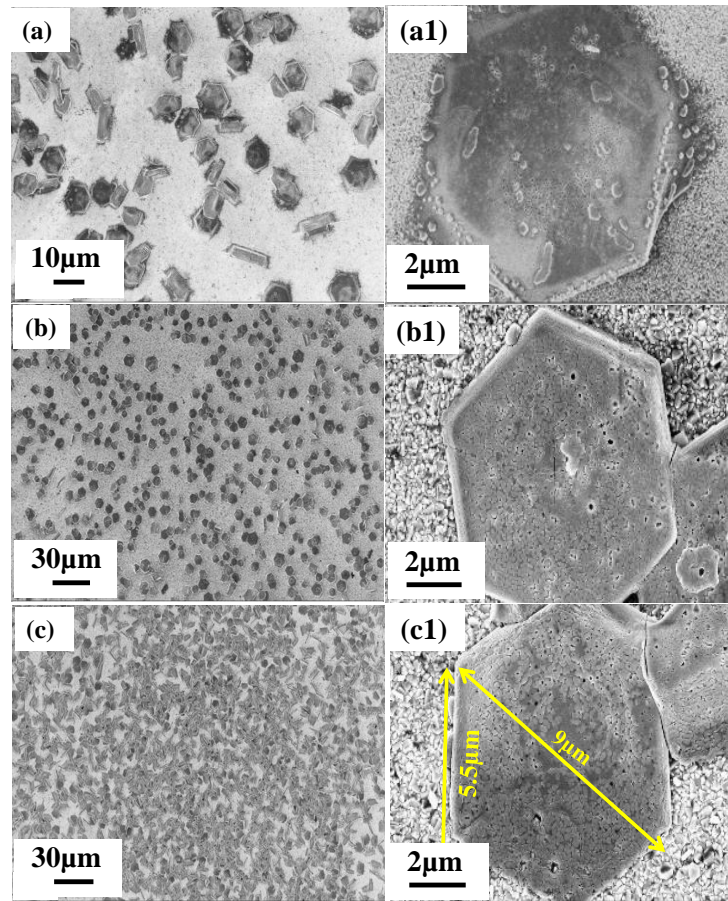


**Figure 4.6** (a) SEM image of MBI with DMSO solvent in 2.25:1.5 concentration, (a1) Enlarged image of (a), (b) SEM image of MBI with DMSO solvent in 1.5:1 concentration, (b1) Enlarged image of (b), (c) SEM image of MBI with DMSO solvent in 3:2 concentration, (c1) Enlarged image of (c)

Figure 4.6 shows morphology of MBI perovskite with DMSO solvent which shows that increasing density with increasing concentration.

### 4.1.3. UV-Vis spectroscopy

We have done comparative analysis through XRD and FESEM

among all those MBI perovskites which were prepared through different solvents and concentration. Seeking a good material property we had selected 3:2 concentrations for all solvent for further analysis. MBI material is using as a light harvester so to analyze the optical property of perovskite. UV-Vis spectroscopy has been done through in two different cases. First Absorption Spectra has been analyzed for MBI solution with different solvents. Absorption spectra has also been analyzed for a thin film after coating and Tauc plot is plotted for different solvents and MBI has excellent absorbing properties (Figure 4.8). They show a direct band gap.

#### 4.1.3.1 UV-Vis spectroscopy for solution:

UV-Vis spectrum was illustrated for MBI solutions in 3:2 concentrations with different solvents between 400 and 900 nm it shows a broad range of absorption in visible range.

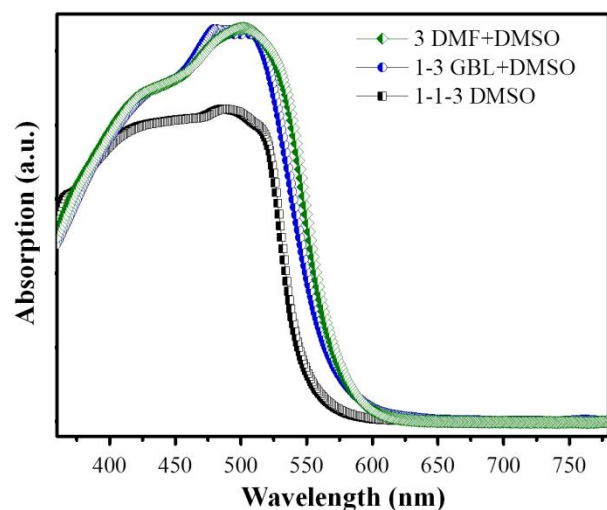
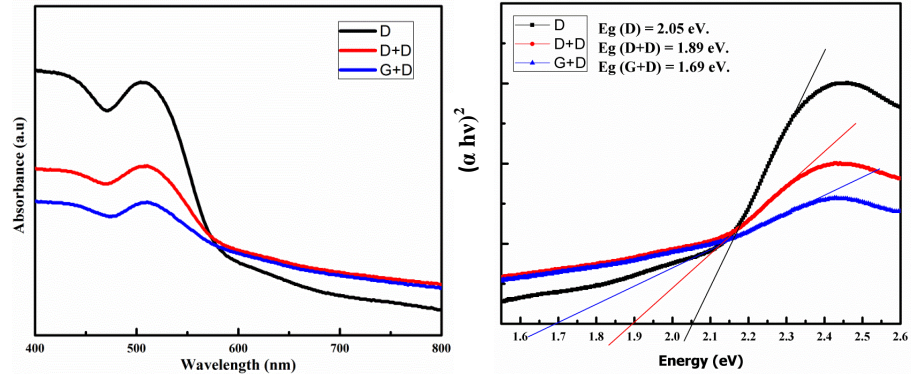


**Figure 4.7:** Absorption spectra for MBI perovskite solutions

#### 4.1.3.2 UV-Vis spectroscopy for thin film:

MBI perovskites solutions were coated over compact layer of  $\text{TiO}_2$  and UV-Vis spectrum was illustrated for MBI thin films in 3:2

concentrations with different solvents between 400 and 800 nm it shows a broad range of absorption in visible range.



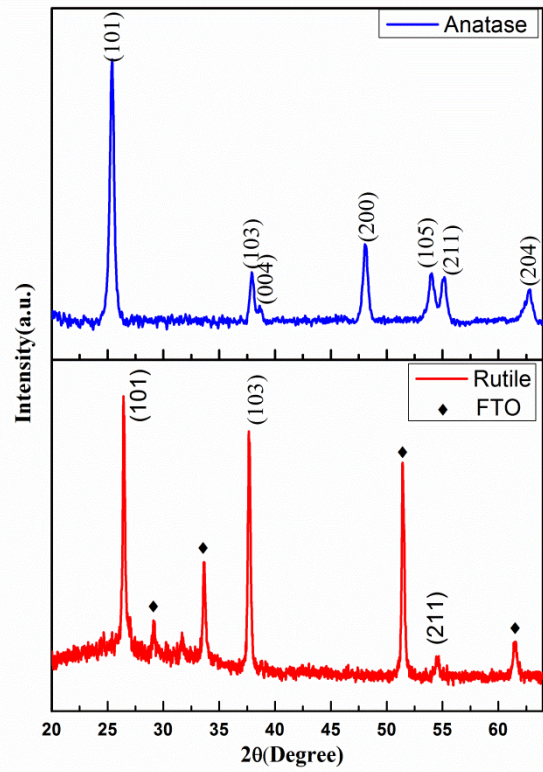
**Figure 4.8:** (a) Absorption spectra for MBI perovskite films, (b) Tauc plot for MBI perovskite films.

Figure 4.8 (a) shows a broad absorption between 400nm to 800nm in visible range. Figure 4.8 (b) shows a Tauc plot for MBI perovskite films. It reveals an optical bandgap of the MBI perovskite at 1.89 eV for first solvent (DMF+DMSO), 1.69eV for solvent (GBL+DMSO), 2.05 eV for solvent (DMSO) as it was derived from a Tauc plot. Some previous report also lies in this range of band gap of MBI [44].

## 4.2 Analysis of TiO<sub>2</sub> Layer

### 4.2.1 XRD analysis of TiO<sub>2</sub>

TiO<sub>2</sub> acts as an electron transport layer while fabricating photovoltaic device. A compact layer of TiO<sub>2</sub> is coated over FTO and then it is annealed at 500° C for 30 minute. X-ray diffraction pattern of TiO<sub>2</sub> compact layer has been analyzed in two phases of TiO<sub>2</sub> named Anatase (Before Annealing) and Rutile (After annealing). The values are confirmed with JCPDS Card No (84-1286).



**Figure 4.9:** XRD analysis of TiO<sub>2</sub>

#### 4.2.2 SEM analysis of TiO<sub>2</sub> compact layer

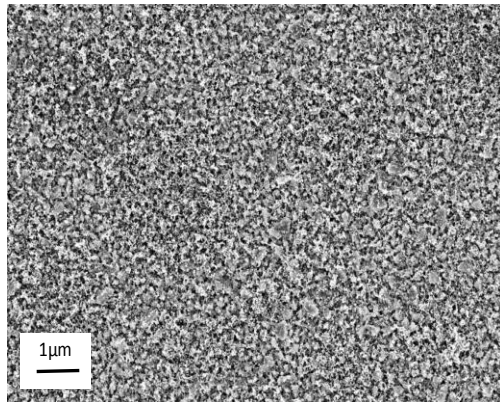


**Figure 4.10:** FESEM analysis of TiO<sub>2</sub> compact layer

Scanning electron microscopy (FESEM) images have been analyzed through Supra55 Zeiss to illustrate about the morphological property of

TiO<sub>2</sub> compact layer. Figure 4.10 shows the compact morphology of TiO<sub>2</sub> thin film coated on FTO substrate [45].

### 4.3 Stability of MBI perovskite:

In order to get appropriate perovskite material for photovoltaic we tried to replace lead with other elements because of some issues like stability, toxicity, etc. Among all choices, we have selected bismuth because it is quite stable rather than lead. To check stability of MBI we had analyzed XRD pattern and SEM images after 10, 20 and 30 days.

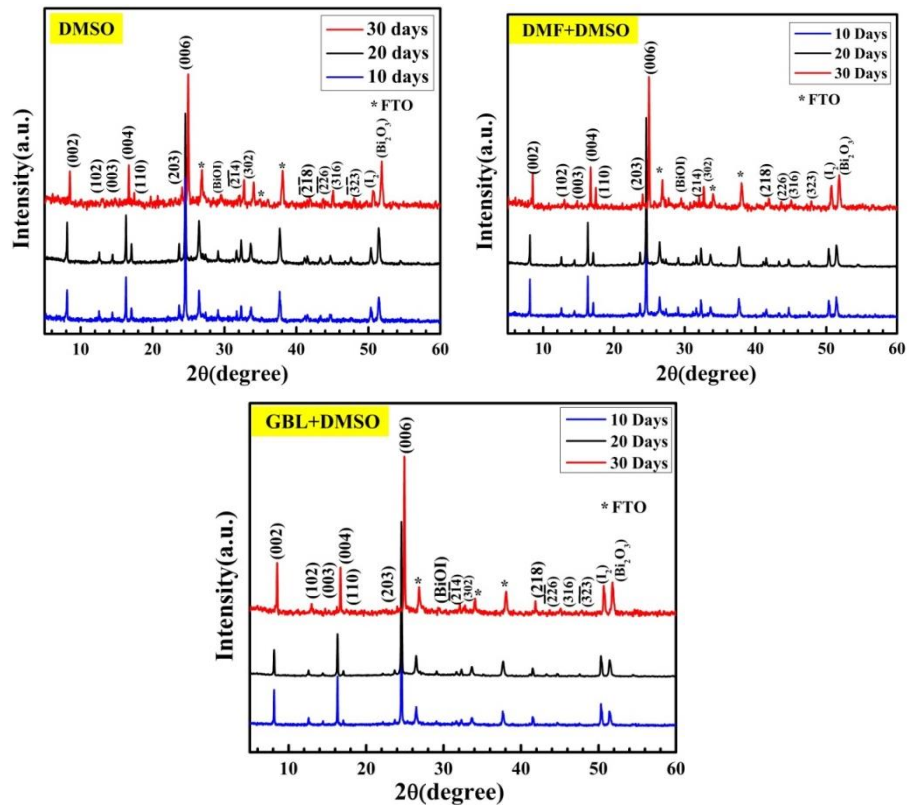


**Figure 4.11:** XRD analysis of MBI with (a) DMSO solvent, (b) DMF+DMSO and (c) GBL+DMSO over a period.

To check the stability XRD pattern have been analyzed after the intervals of 10 days. First we have analyzed after 10 days of

preparation. We found that material is stable but some impurities peak is observed with less intensity. After 20 days intensity of those peaks had been little raised but apart from that perovskite material peak had been observed expectedly which shows stability of bismuth perovskite. Whereas, after 30 days of preparation intensity of impurities have been observed with little increment than previous one. However, peaks of MBI shows quite stability of bismuth perovskite even after 30 days. Somewhat it shows instability of bismuth perovskite over a long time but factor of stability is more rather than lead perovskite.

We compare the air-stability of MBI by exposing it to ambient air. Earlier report shows that  $\text{MAPbI}_3$  changes from brown to yellow after 5 day .By contrast MBI maintains the same visual appearance after 15 days only becoming slightly brighter after 25 days. X-ray diffraction measurements (Figure 4.11) show that the diffraction pattern of MBI remains mostly unchanged.  $\text{MAPbI}_3$ , on the other hand, forms  $\text{PbI}_2$  peaks that become more pronounced over time according to previous work [46].

The small changes to the diffraction pattern of MBI after 10 days and a very little increment can be observed after 20 and 30 days of continuous air exposure. We observed that these changes can be accounted for by the presence of a small quantity of either  $\text{Bi}_2\text{O}_3$  or  $\text{BiOI}$ , which may form on the surface of MBI. Due to high vapor pressure of iodine it may vapor. After annealing iodine molecule is loosely bounded that may cause into tending to vapor. By contrast, most of the  $\text{MAPbI}_3$  transforms to  $\text{PbI}_2$  after 25 days, based on the intensity of the peaks from  $\text{PbI}_2$  vs.  $\text{MAPbI}_3$ .

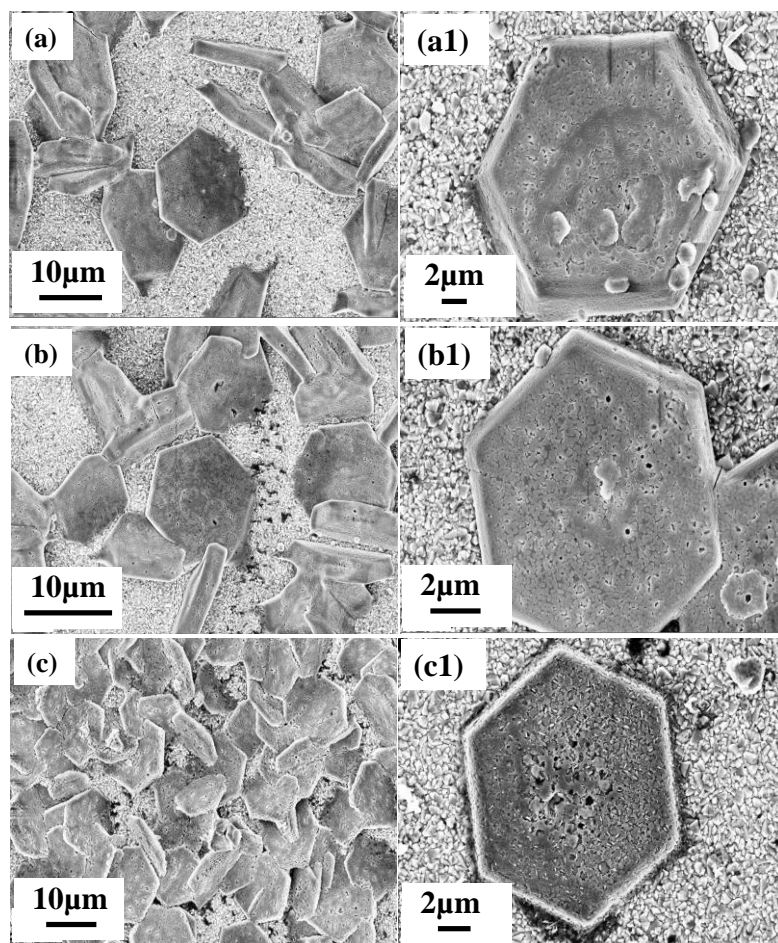


**Figure 4.12:** (a) SEM image of degraded MBI with DMF+DMSO solvent, (a1) enlarged SEM image with DMF+DMSO solvent, (b) SEM image of degraded MBI with DMSO solvent, (b1) enlarged SEM image with DMSO solvent, (c) SEM image of degraded MBI with GBL+DMSO solvent, (c1) enlarged SEM image with GBL+DMSO solvent.

Furthermore, FESEM images have been analyzed after 30 days. We found that over a period of 25-30 days of preparation of the MBI perovskite, the degradation of the material was found. FESEM images from fig 4.12(a) to (c) shows degradation for MBI perovskite for different solvent.

These results suggest that although after the long time MBI degradation also has been started but still MBI is more phase stable

than MAPbI<sub>3</sub> under the testing conditions and forms a thin surface phase after air exposure instead of degrading to BiI<sub>3</sub>.

#### 4.4 I-V measurement:

Efficiency for solar cell (PCE) is denoted by  $\eta$  calculated by using the following formula,

$$\eta = \frac{V_{oc} I_{sc} FF}{P_{in}}$$

$V_{oc}$  is the open-circuit voltage

$I_{sc}$  is the short-circuit current

$FF$  is the fill factor, where  $FF = \frac{V_{max} I_{max}}{V_{oc} I_{sc}}$

$\eta$  is the efficiency

$I$ - $V$  measurements have been carried out by Solar simulator (Photo Emission Tech., Inc., Model-SS50AAA-EM) for MBI perovskite with all three solvents.

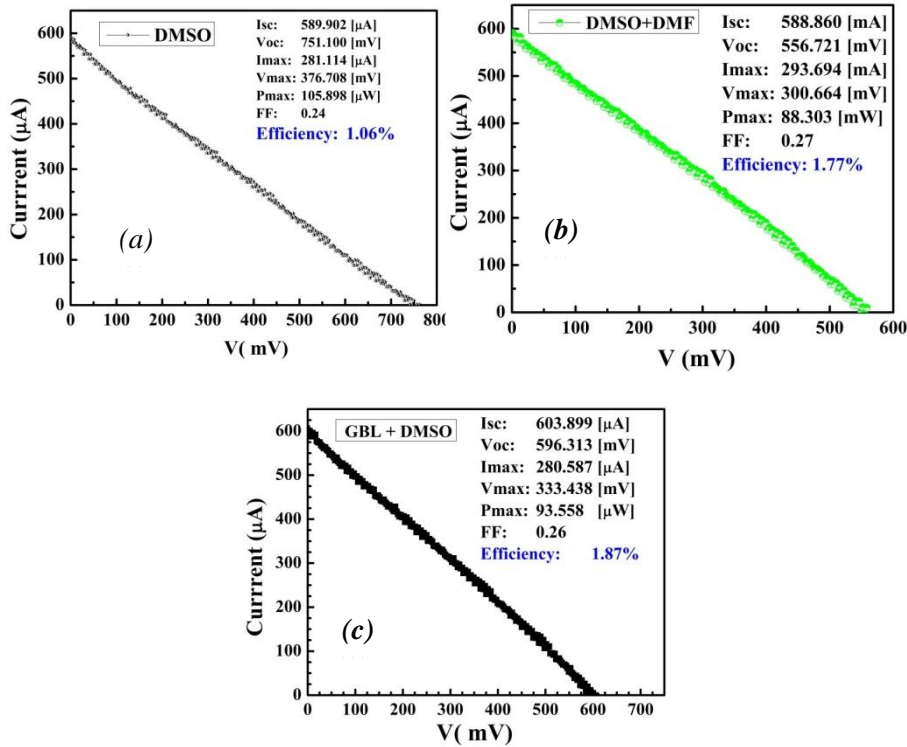


**Figure 4.13:**  $I$ - $V$  measurement for (a) DMSO, (b) DMF+DMSO and (c) GBL+DMSO solvents.

Figure 4.13 shows  $I$ - $V$  measurement for all three solvent. We have got the highest efficiency. For DMSO solvent efficiency is calculated as  $\eta = 1.06\%$ . While for DMF+DMSO solvent it is 1.77% and for GBL+DMSO solvent efficiency is 1.87% with GBL+DMSO solvent. Table 4.1 shows  $I$ - $V$  measurements on the same cell with 10 days intervals. After every measurement the cell was stored under dark to minimize interaction with photons and in ambient atmosphere instead of placing the cells back in glove box. This is done to see how they are reacting when stored in ambient atmosphere.

<b>Time/solvents</b>	<b>DMSO</b>	<b>DMSO + DMF</b>	<b>GBL+DMSO</b>
<b>0 days</b>	1.06%	1.77%	1.87%
<b>10 days</b>	0.94%	1.72%	1.85%
<b>20 days</b>	0.91%	1.68%	1.84%
<b>30 days</b>	0.89%	1.63%	1.83%

**Table 4.1:** Stability test of perovskite solar cells with solvents.

We observed that after 30 days the percentage of efficiency had been decreased by 0.17 and 0.14 in case of DMSO and DMF+DMSO solvent respectively while in case of GBL+DMSO it is decreased by 0.04 only. It shows that MBI perovskite with GBL+DMSO solvent has good stability.



# Chapter 5

## Conclusion and Future scope

---

---

### 5.1 Conclusion:

Here in this project we have synthesized  $(\text{CH}_3\text{NH}_3)_3\text{Bi}_2\text{I}_9$  (MBI) with different solvents and different concentrations. One step solution based process has been used to synthesize MBI. After synthesis we have characterized MBI to study about structural property, morphological and optical property. For structural property XRD pattern have been analyzed for all MBI films with different solvents and concentrations. A comparative analysis has been done among all solvents. We found that in all solvents and concentrations pure phase MBI was synthesized that is inconsistent with previous results. For morphological property we have done FESEM analysis for all solvents and concentrations that show formation of hexagonal structures oriented along the *c*-axis providing an evidence of the formation of MBI perovskites. Interestingly we got a quite dense film for GBL+DMSO solvent. Among all the combination of solvents and concentrations analysis of XRD and FESEM we chose 3:2 concentration for optical analysis due to its better result with all solvents. UV-Vis spectroscopy was done for all solvents. The optical characterization confirms the strong visible absorption of MBI with an optical bandgap of 1.69-2.05 eV. To check the stability of MBI, XRD and FESEM analyses have been done after intervals of 10 days. Degradation can be seen after 25-30 days but dominantly appearance of MBI shows quite stability of MBI perovskites. Finally, attempts

have been made to fabricate a photovoltaic device using the as-prepared MBI to study its photoresponse. We have calculated efficiency 1.06% for DMSO solvent, 1.77% for DMF+DMSO solvent and finally the highest efficiency 1.87%, we have got with GBL+DMSO solvent. We concluded that GBL+DMSO solvent is best among all three solvents. Stability is also found best with GBL+DMSO solvent.

## **5.2 Future Scope:**

Perovskites have to be studied more in the field of optoelectronics. Perovskites have drawn attention especially in photovoltaics. So far, lead perovskites have emerged with significant efficiency but lead free perovskite has to be reached up to significant mark. Regarding more study and research has to be done. It would be interesting to investigate what makes the perovskite solar cells degrade during constant illumination to discover a way to prevent it. Because that is the biggest obstacle right now for making them commercialized. It would also be interesting to investigate alternative materials for every layer in the PSC structure, to try to optimize the cell and see if other materials reduce degradation.

There are still many unknown details around the PSC and this thesis might have raised more questions than given answers. Still it might set an opportunity for further research that could lead to answer the following questions raised during this research. Is this the best PSC structure? Could other materials for ETL, HTL and active layer be better? Can Au be replaced? It would be interesting to investigate different PSC structures and experiment with different layers, to see if another structure has better stability, PCE and to minimize the use of finite and toxic materials. Like change FTO to ITO, try another perovskite without lead and maybe replace Au electrode. We can use double perovskites according to electronic configuration also and see

how much they are efficient.

In addition, a rapid research going on tandem solar cell in photovoltaics. Perovskite is being used in tandem solar cell [47]. Organometal-halide perovskite/Si tandem solar cells (TSCs) have been proposed as a promising candidate to surpass Si efficiency records. Their power conversion efficiency has rapidly increased.

## References:

1. A. Navrotsky "Energetics and Crystal Chemical Systematics among Ilmenite, Lithium Niobate, and Perovskite Structures". Chem. Mater. , vol. 10, no.10, pp. 2787,1998.
2. Mats Johansson and Peter Lemmens "Crystallography and Chemistry of Perovskites", Handbook of Magnetism and Advanced Magnetic Materials, John Wiley & Sons, 2007.
3. NPTELlectures([http://nptel.ac.in/courses/113104005/lecture4/4\\_2.htm](http://nptel.ac.in/courses/113104005/lecture4/4_2.htm)).
4. Robert S. Roth" Classification of Perovskite and Other  $ABO_3$ -Type Compounds", Journal of Research of the National Bureau of Standards "vol. 58, No.2, February 1957.
5. M. M. Lee, J. Teuscher, T. Miyasaka, T. N. Murakami, and H. J. Snaith, "Efficient hybrid solar cells based on meso-structured organometal halide perovskites," Science, vol. 338, no. 6107, pp. 643-647, 2012.
6. A. O'regan and M Grfitzeli, "A low-cost, high-efficiency solar cell based on dye-sensitized," nature, vol. 353, no. 6346, pp. 737-740, 1991.
7. A. Kojima, K. Teshima, Y. Shirai, and T. Miyasaka, "Organometal halide perovskites as visible-light sensitizers for photovoltaic cells," Journal of the American Chemical Society, vol. 131, no. 17, pp. 6050-6051, 2009.
8. X. Li, D.Bi, C.Yi, J.-D. Decoppet, J. Luo, S. M. Zakeeruddin, A. Hagfeldt, and M. Gratzel, "A vacuum flash-assisted solution process for high-efficiency large-area perovskite

- solar cells," *Science*, vol. 353, no. 6294, pp. 5862, 2016.
9. A. M. Ganose, C. N. Savory, and D. O. Scanlon, "Beyond methylammonium lead iodide: Prospects for the emergent field of  $ns^2$  containing solar absorbers," *Chemical Communications*, vol. 53, no. 1, pp. 20-44, 2017.
  10. T. Singh, A. Kulkarni, M. Ikegami, and T. Miyasaka, "Effect of electron transporting layer on bismuth-based lead-free perovskite  $(CH_3NH_3)_3 Bi_2I_9$  for photovoltaic applications," *ACS applied materials & interfaces*, vol. 8, no. 23, pp. 14 542-14 547, 2016.
  11. B.W. Park, B. Philippe, X. Zhang, H. Rensmo, G. Boschloo, and E. M. Johansson, "Bismuth based hybrid perovskites  $A_3B_2I_9$  (A: Methylammonium or cesium) for solar cell application," *Advanced Materials*, vol. 27, no. 43, pp. 6806-6813, 2015.
  12. H.-S. Kim, C.-R. Lee, J.-H. Im, K.-B. Lee, T. Moehl, A. Marchioro, S.-J. Moon, R. Humphry-Baker, J.-H. Yum, J. E. Moser, *et al.*, "Lead iodide perovskite sensitized all-solid-state submicron thin film mesoscopic solar cell with efficiency exceeding 9%," *Scientific reports*, vol. 2, pp. 591, 2012.
  13. J. H. Noh and S. I. Seok, "Steps toward efficient inorganic-organic hybrid perovskite solar cells," *MRS Bulletin*, vol. 40, no. 08, pp. 648-653, 2015.
  14. M. A. Green, K. Emery, Y. Hishikawa, W. Warta, and E. D. Dunlop, "Solar cell efficiency tables (version 46)," *Progress in Photovoltaics: Research and Applications*, vol. 23, no. 7, pp. 805-812, 2015.
  15. U.NREL, Best efficiency cell review <https://www.nrel.gov/pv/>.
  16. H. J. Snaith, "Perovskites: The emergence of a new era for

- low-cost, high efficiency solar cells," *The Journal of Physical Chemistry Letters*, vol. 4, no. 21, pp. 3623-3630, 2013.
17. K. Momma and F. Izumi, "Vesta 3 for three-dimensional visualization of crystal, volumetric and morphology data," *Journal of Applied Crystallography*, vol. 44, no. 6, pp. 1272-1276, 2011.
  18. Z. Zhang, X. Li, X. Xia, Z. Wang, Z. Huang, B. Lei, and Yun Gao "High-Quality  $(\text{CH}_3\text{NH}_3)_3\text{Bi}_2\text{I}_9$  Film-Based Solar Cells: Pushing Efficiency up to 1.64%" *J. Phys. Chem. Lett.*, vol. 8, pp. 4300–4307, 2017.
  19. K. Eckhardt, V. Bona, J. Getzschmann, J. Grothe, F. Wissera and S. Kaskel "Crystallographic insights into  $(\text{CH}_3\text{NH}_3)_3(\text{Bi}_2\text{I}_9)$ : A new lead-free hybrid organic-inorganic material as a potential absorber for photovoltaics" *ChemComm.*, vol. **52**, pp. 3058-3060, 2016.
  20. T.-B. Song, Q. Chen, H. Zhou, C. Jiang, H.-H. Wang, Y. M. Yang, Y. Liu, J. You, and Y. Yang, "Perovskite solar cells: Film formation and properties," *Journal of Materials Chemistry A*, vol. 3, no. 17, pp. 9032-9050, 2015.
  21. D.-J. Kwak, B.-H. Moon, D.-K. Lee, C.-S. Park and Y.-M. Sung, "Comparison of transparent conductive indium tin oxide, titanium-doped indium oxide, and uridine-doped tin oxide films for dye-sensitized solar cell application," *Journal of Electrical Engineering and Technology*, vol. 6, no. 5, pp. 684-687, 2011.
  22. T. Dittrich, F. Lang, O. Shargaieva, J. Rappich, N. Nickel, E. Unger, and B. Rech, "Diffusion length of photo-generated charge carriers in layers and powders of  $\text{CH}_3\text{NH}_3\text{PbI}_3$  perovskite," *Applied Physics Letters*, vol. 109, no. 7, pp. 073901(1-4), 2016.
  23. <http://www.thesolarspark.co.uk/the-science/solar-power/thin->

film/perovskite-solar-cells.

24. A. Paulke, S. D. Stranks, J. Kniepert, J. Kurpiers, C. M. Wol, N. Schon, H. J. Snaith, T. J. Brenner, and D. Neher, "Charge carrier recombination dynamics in perovskite and polymer solar cells," *Applied Physics Letters*, vol. 108, no. 11, pp. 113 505 (1-5), 2016.
25. REN21, Renewables 2017 global status report, <http://www.ren21.net>
26. W.J. Yin, J.-H. Yang, J. Kang, Y. Yan, and S.-H. Wei, "Halide perovskite materials for solar cells: A theoretical review," *Journal of Materials Chemistry A*, vol. 3, pp. 8926-8942, 2015.
27. Kojima, Akihiro, Teshima, Kenjiro, Shirai, Yasuo, Miyasaka, Tsutomu. "Organometal Halide Perovskites as Visible-Light Sensitizers for Photovoltaic Cells". *Journal of the American Chemical Society*, vol. 131, no. 17, pp. 6050–6051, 2009.
28. Im, Jeong-Hyeok; Lee, Chang-Ryul Lee, Jin-Wook Park, Sang-Won Park, Nam-Gyu (2011). "6.5% efficient perovskite quantum-dot-sensitized solar cell". *Nanoscale*, vol. 3, no. 10, pp. 4088–93, 2011.
29. Lee, M. M. Teuscher, J. Miyasaka, T. Murakami, T. N. Snaith, H. J. "Efficient Hybrid Solar Cells Based on Meso-Structured Organometal Halide Perovskites". *Science*. vol. 338, no. 6107, pp. 643–647, 2012.
30. Hadlington, Simon (October 4, 2012). "Perovskite coat gives hybrid solar cells a boost". *RSC Chemistry world*, 2012.
31. Kim, Hui-Seon Lee, Chang-Ryul Im, Jeong-Hyeok Lee, Ki-Beom Moehl, Thomas Marchioro, Arianna Moon, Soo-Jin Humphry-Baker, Robin Yum, Jun-Ho Moser, Jacques E. Grätzel, Michael Park, Nam-Gyu "Lead Iodide Perovskite Sensitized All-Solid-State Submicron Thin Film Mesoscopic

- Solar Cell with Efficiency Exceeding 9%". *Scientific Reports*. vol. 2, no. 591(1-5), 2012.
32. Liu, Mingzhen Johnston, Michael B. Snaith, Henry J. (2013). "Efficient planar heterojunction perovskite solar cells by vapour deposition". *Nature*, vol. 501, no.7467, pp. 39(5–8), 2013.
33. Ball, James M. Lee, Michael M. Hey, Andrew Snaith, Henry J. "Low-temperature processed meso-superstructured to thin-film perovskite solar cells". *Energy & Environmental Science*. Vol. 6, no. 6, pp. 1739, 2013.
34. Eperon, Giles E. Burlakov, Victor M. Docampo, Pablo Goriely, Alain Snaith, Henry J." Morphological Control for High Performance, Solution-Processed Planar Heterojunction Perovskite Solar Cells". *Advanced Functional Materials*, vol. 24, no, 1, pp. 151–157, 2014.
35. Saliba, Michael Tan, Kwan Wee Sai, Hiroaki Moore, David T. Scott, Trent Zhang, Wei Estroff, Lara A. Wiesner, Ulrich Snaith, Henry J.. "Influence of Thermal Processing Protocol upon the Crystallization and Photovoltaic Performance of Organic–Inorganic Lead Trihalide Perovskites". *The Journal of Physical Chemistry C*. vol. 118, no. 30, pp. 17171–17177, 2014.
36. Tan, Kwan Wee Moore, David T. Saliba, Michael Sai, Hiroaki Estroff, Lara A. Hanrath, Tobias Snaith, Henry J. Wiesner, Ulrich . "Thermally Induced Structural Evolution and Performance of Mesoporous Block Copolymer-Directed Alumina Perovskite Solar Cells". *ACS Nano*. vol. 8, no. 5, pp. 4730–4739, 2014.
37. Liu, Mingzhen Johnston, Michael B. Snaith, Henry J. "Efficient planar heterojunction perovskite solar cells by vapor deposition". *Nature*. vol. 501, no. 7467, pp. 395–398,

- 2013.
38. <https://www.theguardian.com/technology/2014/mar/02/perovskite-lightbulb-moment-abundant-solar-power-britain> "The Guardian: "The perovskite lightbulb moment for solar power".
  39. Docampo, Pablo, Ball, James M. Darwich, Mariam Eperon, Giles E. Snaith, Henry J. "Efficient organometal trihalide perovskite planar-heterojunction solar cells on flexible polymer substrates". *Nature Communications*. vol.4, pp. 2761, 2013.
  40. Zhou, H. Chen, Q. Li, G. Luo, S. Song, T. B. Duan, H.S. Hong, Z. You, J. Liu, Y. Yang, Y. "Interface engineering of highly efficient perovskite solar cells". *Science*. vol.345, no.6196, pp. 542–546, 2014.
  41. K. Eckhardt, V. Bon, J. Getzschmann, J. Grothe, F. M. Wisser, and S. Kaskel, Crystallographic insights into  $(\text{CH}_3\text{NH}_3)_3(\text{Bi}_2\text{I}_9)$ : A new lead-free hybrid organic-inorganic material as a potential absorber for photovoltaics," *Chemical Communications*, vol. 52, no. 14, pp. 3058-3060, 2016.
  42. A. Kojima, *et al.*, Organometal Halide Perovskites as Visible-Light Sensitizers for Photovoltaic Cells. vol. 131, pp. 17, 2009.
  43. H. S. Jung and N. G. Park, Perovskite Solar Cells: From Material to Devices. *Small*, vol. 11, pp.10- 25, 2015.
  44. M. Pazoki, M. B. Johansson, H. Zhu, P. Broqvist, T. Edvinsson, G. Boschloo, and E. M. J. Johansson "Bismuth Iodide Perovskite Materials for Solar Cell Applications: Electronic Structure, Optical Transitions, and Directional Charge Transport" *J. Phys. Chem. C*, vol. 120, pp. 29039–29046, 2016.
  45. M. M. Lee, J. Teuscher, T. Miyasaka, T. N. Murakami, and

- H. J. Snaith, Efficient hybrid solar cells based on meso-structured organometal halide perovskites," *Science*, vol. 338, no. 6107, pp. 643-647, 2012.
46. B. W. Park , B. Philippe, X. Zhang , H. Rensmo, G. Boschloo and E. M. J. Johansson "Bismuth Based Hybrid Perovskites  $A_3Bi_2I_9$ (A: Methylammonium or Cesium) for Solar Cell Application" *Adv. Mater*, vol. 27, pp. 6806–6813, 2015.
47. M. H. Futscher and B. Ehrler "Efficiency Limit of Perovskite/Si Tandem Solar Cells" *ACS Energy Lett.*, vol. 1, no. 4, pp. 863–868, 2016.